(12) LEVEL III

A106686

RADC-TR-81-241
Final Technical Report
September 1981

ACOSS SEVEN (ACTIVE CONTROL OF SPACE STRUCTURES)

General Dynamics/Convair Division

Sponsored by
Defense Advanced Research Projects Agency (DoD)
ARPA Order No. 3654

ROME AIR DEVELOPMENT CENTER
Air Force Systems Command
Griffiss Air Force Base, New York 13441

This report has been reviewed by the RADC Public Affairs Office (PA) and is releasable to the National Technical Information Service (NTIS). At NTIS it will be releasable to the general public, including foreign nations.

RADC-TR-81-241 has been reviewed and is approved for publication.

APPROVED: Richard W. Carman

RICHARD W. CARMAN
Project Engineer

APPROVED: Mylan A. Haugen

MYLAN A. HAUGEN, Colonel, USAF
Chief, Surveillance Division

FOR THE COMMANDER: John P. Huss

JOHN P. HUSS
Acting Chief, Plans Office

If your address has changed or if you wish to be removed from the RADC mailing list, or if the addressee is no longer employed by your organization, please notify RADC (OCSE) Griffiss AFB NY 13441. This will assist us in maintaining a current mailing list.

Do not return copies of this report unless contractual obligations or notices on a specific document requires that it be returned.

ACOSS SEVEN (ACTIVE CONTROL OF SPACE STRUCTURES)

John R. Sesak

Contractor: General Dynamics Convair Division
Contract Number: F30602-80-C-0164
Effective Date of Contract: 17 April 1980
Contract Expiration Date: 19 December 1980
Short Title of Work: Acoss Seven (Active Control of Space Structures)
Program Code Number: OE20
Period of Work Covered: Apr 80 - Dec 80

Principal Investigator: Johns R. Sesak
Phone: 714 277-8900 x 1739

Project Engineer: Richard W. Carman
Phone: 315 330-3148

This research was supported by the Defense Advanced Research Projects Agency of the Department of Defense and was monitored by Richard W. Carman (RADC/OCSE), Griffiss AFB NY 13441 under Contract F30602-80-C-0164.

UNCLASSIFIED

SECURITY CLASSIFICATION OF THIS PAGE (When Data Entered)

REPORT DOCUMENTATION PAGE

READ INSTRUCTIONS BEFORE COMPLETING FORM

1. REPORT NUMBER: RADC-TR-81-241	2. GOVT ACCESSION NO.: AD-A106 687
3. RECIPIENT'S CATALOG NUMBER:	
4. TITLE (and Subtitle): ACOSS SEVEN (ACTIVE CONTROL OF SPACE STRUCTURES)	5. TYPE OF REPORT & PERIOD COVERED: Final Technical Report 17 Apr 80 - 19 Dec 80
	6. PERFORMING ORG. REPORT NUMBER:
7. AUTHOR(s): John R. Sesak	8. CONTRACT OR GRANT NUMBER(s): F30602-80-C-0164, ARPA Order-3634
9. PERFORMING ORGANIZATION NAME AND ADDRESS: General Dynamics, Convair Division, P. O. Box 80847, San Diego CA 92138	10. PROGRAM ELEMENT, PROJECT, TASK AREA & WORK UNIT NUMBERS: 62301E, C6540107, 17 02
11. CONTROLLING OFFICE NAME AND ADDRESS: Defense Advanced Research Projects Agency, 1400 Wilson Blvd., Arlington VA 22209	12. REPORT DATE: September 1981
	13. NUMBER OF PAGES: 108
14. MONITORING AGENCY NAME & ADDRESS (if different from Controlling Office): Rome Air Development Center (OCSE), Griffiss AFB NY 13441	15. SECURITY CLASS. (of this report): UNCLASSIFIED
	15a. DECLASSIFICATION/DOWNGRADING SCHEDULE: N/A

16. DISTRIBUTION STATEMENT (of this Report)

Approved for public release; distribution unlimited.

17. DISTRIBUTION STATEMENT (of the abstract entered in Block 20, if different from Report)

Same

18. SUPPLEMENTARY NOTES

RADC Project Engineer: Richard Carman (OCSE)

19. KEY WORDS (Continue on reverse side if necessary and identify by block number)

Large Space Systems	Model Error Sensitivity Suppression
Structural Damping Augmentation	Filter Accommodation
Modern Modal Control	Disturbance Accommodation

20. ABSTRACT (Continue on reverse side if necessary and identify by block number)

This report covers active structural control theory extensions, simulations, and demonstration test planning as they relate to precision control of large space systems. Theory material includes a filter accommodation technique for stabilizing higher modes without degrading controlled mode performance, Liapunov stability analysis, and disturbance accommodation techniques for systems where damping along cannot meet requirements.

DD FORM 1 JAN 73 1473 EDITION OF 1 NOV 65 IS OBSOLETE

UNCLASSIFIED

SECURITY CLASSIFICATION OF THIS PAGE (When Data Entered)

TABLE OF CONTENTS

TABLE OF CONTENTS, Contd

LIST OF FIGURES

LIST OF FIGURES, Contd

LIST OF FIGURES, Contd

LIST OF TABLES

SECTION 1

INTRODUCTION

1.1 SUMMARY

This report covers the work performed by General Dynamics on the Active Control of Space Structures (ACOSS SEVEN) program. The objective of ACOSS SEVEN was to extend and refine General Dynamics' modern control theory approach Model Error Sensitivity Suppression (MESS) and thus provide a unified dynamics and control technology base for large spaceborne structures requiring stringent line of sight (LOS) requirements. Additional objectives were analysis and simulation and demonstration test planning.

The problem of achieving comprehensive control of large spaceborne structures is essentially one of model error. A control system must be designed for a truncated model of an essentially infinite-order system. The truncated modes fall into two classes: known and unknown. The known modes are easily handled through the MESS algorithm by a simple alteration of the optimal performance index. To cope with the problem of model error caused by the truncation of unknown high frequency residual modes, General Dynamics, during the course of the study, developed the filter accommodation algorithm. Filter Accommodated Optimal Control allows the design of low bandwidth optimal control and estimation systems such that the unknown high frequency residual modes are gain stabilized. Filter accommodation allows the inclusion of a-priori designer specified low frequency filter dynamics in the control loop such as Tchebycheff or Butterworth; the optimal control law is designed specific to the chosen filter dynamics such that the low pass characteristics of the compensator loop are not nullified. The algorithm allows filter attenuation to begin within the control system bandwidth, the controller essentially works through the filter, and low-order filters may be used to achieve the required degree of residual mode attenuation. Filter accommodation is compatible with the basic MESS algorithm. Simultaneous use of both algorithms - Filter Accommodated Model Error Sensitivity Suppression (FAMESS) provides simultaneous alleviation of the truncation problems of LSS control; i.e., the suppression and attenuation of model error caused by the truncation of known and unknown modes.

In the area of overall system stability a Liapunov stability analysis was performed for the filter accommodated designs. A stability criteria was developed which is a function of residual mode parameters and compensator gain levels.

The Draper Evaluation Structure #2 was analyzed and disturbance accommodation techniques in conjunction with decoupled control were applied to meet the LOS error specifications.

As part of the Demonstration Planning task, various large space structure conceptual designs were surveyed to identify the types of structural element used. These elements were then put into a versatile test structure design which includes provision to vary structural stiffness.

1.2 RECOMMENDATIONS

The MESS/FAMESS control technique has demonstrated significant progress toward the goal of a generic, unified control methodology for large spaceborne structures with stringent stabilization and control requirements: The truncation and attendant spillover problems for LSS control by Linear Quadratic Gaussian (LQG) methods are essentially resolved. As a result of our ACOSS work, one can now routinely design finite dimensional LQG controllers for infinite dimensional systems employing a systematic methodology.

However some additional progress is required before the control theory requirements can be declared fulfilled for all classes of systems operating in all disturbance environments. The resolution of the fundamental modal truncation problems permit attention to be directed toward measures of system performance and merit; i.e., gain margins, phase margins, system sensitivity, robustness, disturbance rejection and model reduction. It makes little engineering sense to expend a large amount of time and effort on these questions before the basic issues of modal truncation are formally resolved. In addition to the control issues just enumerated, as technology moves toward actual hardware implementation a host of design interface and integration problems appear; i.e., just how does one distribute the damping requirements among the structural design process, passive damping devices, and the active control system in a systematic procedure such that the overall system is truly integrated and no damping technique is considered in ad hoc fashion. The following areas are recommended for additional study.

1.2.1 THEORY EXTENSION.

Stability Margins: The Liapunov stability results obtained thus far are functions of the residual mode parameters. One obtains stability results as functions of worst case parameters. This approach, while sufficient for some systems, may be inapplicable or cumbersome for others. Thus some attempt should be made to develop stability margins that are not dependent on unknown modal parameters.

In addition, now that the truncation problems are resolved, classical gain and phase margin concepts should be generalized to multivariable control and applied to the LSS control problem. Many such results exist as isolated facts in the literature, but as usual, these results must be modified and melded together to provide a useful design methodology.

System Robustness: The closed-loop robustness properties of LQG designs is ultimately tied to the optimal compensator. General Dynamics made significant progress on the compensator question via its constrained compensator algorithm during ACOSS Phase Ia; however, recently developed singular value robustness measures should be modified, as necessary, and incorporated into the FAMESS design methodology such that the compensator which emerges from the design process has a prescribed degree of robustness as measured by the singular value criterion.

Disturbance Rejection: Disturbance rejection techniques must be suitably modified to be useful for LSS control. Disturbance site estimation and feedforward control is recommended to cancel disturbance effects whenever possible. This preference is for two reasons: first, the finite propagation time entailed by the distributed nature of large space systems could permit the disturbance process to be operational for long periods of time before it was detected at nominal system outputs. Estimation of the disturbance process at the disturbance site eliminates this possibility. Secondly, the feedforward control technique provides a two degree of freedom control system such that the disturbance accommodating loop can be designed independently of the modal damping loop.

The Draper Evaluation Structure Number 2 provides an outstanding example of the need for the development of disturbance accommodation technology suitable for LSS control. No amount of modal damping will permit the system to meet LOS requirements. Thus one must develop additional control technology which is compatible with modal damping technique of the active control system. It is again noted that the development of these secondary control technologies for LSS control was impossible until the truncation problems were resolved.

Closed-Loop Model Reduction: Some means of controller simplication should be attempted; i.e., one first designs the high order controller and then systematically eliminates controlled states and readjusts system gains to maintain performance. The end result of this process is a high performance controller of reduced complexity.

1.2.2 ROLE OF DISTURBANCE ACCOMMODATION

The Draper Evaluation Structure #2 raises the question of the relative roles of active structural damping and disturbance accommodation. Although active structural damping technology has received by far most of the emphasis in prior active structural control work, the Draper Evaluation Structure #2 could not be made sufficiently quiet to meet specifications by the application of active damping. Thus it is recommended that studies be performed to establish whether disturbance accommodation technology should receive increased emphasis or whether the Evaluation Structure presents a problem which is best solved by structural design changes.

1.2.3 STRUCTURAL CONTROL COMPONENTS

Reviews of the active structural control state of the art clearly indicate that control theory is far ahead of practical implementation. Except for a few cases, active structural control test work has used actuators and/or sensors which are not applicable to use on real structures in space. Thus additional theory developments are certainly important but increased emphasis on practical control system implementation appears to be essential if the active structural control technology is to be ready to support large space systems in a timely manner.

SECTION 2

CONTROL THEORY

A systematic procedure for handling the truncation of unknown high frequency residual modes has long been an open problem in Large Space System (LSS) control, (References 1-6). Residual modes are those vibration modes that are neglected during the design process. These modes are usually poorly known and of high frequency. (The precision of modal calculations decreases as modal frequency increases.) This problem of unknown dynamic characteristics at high frequencies is endemic throughout control engineering and is not generic to the LSS control problem specifically. The designer rarely knows the high frequency characteristics of the plant; however, due to the infinite series, modal representation of large space systems, the problem of unknown high frequency modal dynamics is more visible and plays a greater part in the LSS design process than in many other control systems.

Classically, the usual technique to cope with unknown dynamics at high frequencies has been the roll-off filter, i.e., loop gain decreases as frequency increases, and thus all dynamics above a certain frequency are gain stabilized, (Reference 7). This is the approach that we shall adopt here; however, this roll-off filter concept is not easily applied in optimal control and estimation systems, which are generally high bandwidth systems. Thus, we develop a new specific optimal control algorithm that permits the inclusion of designer selected filter dynamics. The primary reason for this roll-off filter approach stems from the uncertainty of LSS plant dynamics at high frequencies. Ultimately, we know nothing about the high frequency modes; neither mode shape nor frequency. Such lack of knowledge precludes a precise mathematical formulation of the problem. (Recall that characteristics of sensors and actuators, both physical devices, are not known with great precision at high frequencies.)

Thus we adopt the roll-off filter approach and attenuate what we do not know. However, this roll-off filter approach must be further modified for LSS control because of the extremely dense modal spectrum of the LSS. As illustrated in Figure 2-1, the previous approach for small satellites was the design of low bandwidth controllers and a stiff structure such that all flexible body modes were outside the control system bandwidth, but this approach is not feasible for large systems where the vibration modes are fractions of a Hertz and frequency separations are on the order of a one-one hundredth of a Hertz. Thus we must not only attenuate residual modal response, but must actually design a controller that works through the filtering system such that certain modes deemed critical to the control task are controlled and the responses from unknown residual modes are attenuated.

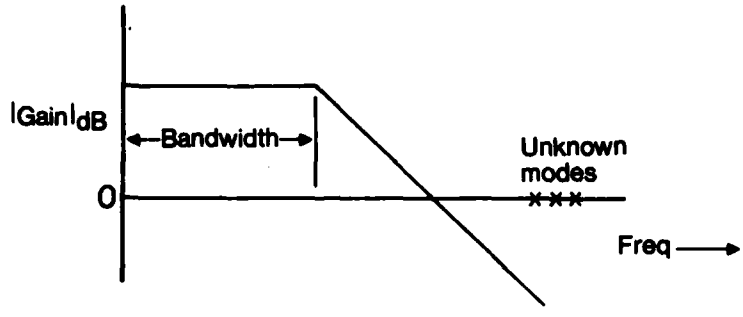

15061275-32

Figure 2-1. Classical Clósed-Loop Control Approach

2.1 THE LSS CONTROL PROBLEM

The LSS control problem can be sufficiently described by recourse to three state space spacecraft models: the evaluation model, the design model, and the control model, (Reference 8).

2.1.1 EVALUATION MODEL. This is the most complex model and has the closest fidelity to the actual physical system. This model is used to validate the closed-loop system after design and usually encompasses unknown modes, disturbances, and non-linearities. In actuality, the evaluation model can be any set of dynamic equations that can be placed on a computer. Figure 2-2 characterizes a typical linear high-order evaluation model that is employed to evaluate truncation error sensitivity.

The following definitions apply to the partioned equations:

Controlled states: $x_c \in R^n$

Suppressed states: $x_s \in R^s$

Residual states: $x_r \in R^r$

Control vector: $u \in R^m$

Observation vector: $y \in R^1$

Control spillover: $B_s u$ and $B_r u$

Observation spillover: $C_s x_s$ and $C_r x_r$

$$\begin{bmatrix} \dot{x}_C \\ \dot{x}_S \\ \dot{x}_r \end{bmatrix} = \begin{bmatrix} A_C & 0 & 0 \\ 0 & A_S & 0 \\ 0 & 0 & A_r \end{bmatrix} \begin{bmatrix} x_C \\ x_S \\ x_r \end{bmatrix} + \begin{bmatrix} B_C \\ B_S \\ B_r \end{bmatrix} [u]$$

$$[y] = \begin{bmatrix} C_C & C_S & C_r \end{bmatrix} \begin{bmatrix} x_C \\ x_S \\ x_r \end{bmatrix}$$

The residual state vector x_r is of arbitrary dimension.

10129615-98A

Figure 2-2. Evaluation Model

The plant matrix has the block diagonal form shown because the state variables characterize modal coordinates.

This partition of the state vector reflects control objectives and modeling accuracy. The controlled states, x_c, characterize those critical modes that must be controlled to achieve satisfactory system performance. The suppressed states, x_s, characterize those modes whose control is not critical to the control task. The suppressed modes are well known, but do not greatly influence the control objective. It is desirable to eliminate these modes from the dynamic model in order to minimize system complexity. The residual states, x_r, characterize unknown or unreliably computed modes. The residual modes are usually of high frequency and are neglected during the design process. These residual modes, however poorly known, do constitute system characteristics with which the design process must cope. It is these residual states that will receive primary emphasis in this development.

The spillover terms indicate undesirable effects of reduced-order control system design. Control spillover is the excitation of uncontrolled modes by the controller, and observation spillover is the sensing of uncontrolled modal responses by the observer. In a closed-loop system, simultaneous control and observation spillover can cause instability, (References 5, 6). Thus, spillover reduction is one objective for low-order control of high-order systems.

2.1.2 DESIGN MODEL. This model contains states corresponding to those modes that can be reliably computed and can be viewed as a truncated version of the evaluation model, Figure 2-2, with the residual states deleted. Figure 2-3 characterizes the typical linear design model. The design model usually contains too many states to be actively controlled. Also, many of the states labeled x_s are not critical to the performance objectives; thus, the design model is further truncated.

2.1.3 CONTROL MODEL. This model contains those states that correspond to critical modes that must be controlled to meet performance requirements. Figure 2-4 characterizes the typical linear control model.

If an identity estimator is employed in the system design, the low-order control model yields a model for the estimator.

2.1.4 LSS CONTROL PROBLEM. The LSS control problem now can be cast simply as: design a controller that stabilizes the control model, Figure 2-4, remains stable, and meets performance criteria when applied to the evaluation model, Figure 2-2.

Alternately we pose the question: is it possible to design a controller based on the dynamic system x_c, and suppress sensitivity to modeling errors deliberately

$$\begin{bmatrix} \dot{x}_C \\ \dot{x}_S \end{bmatrix} = \begin{bmatrix} A_C & 0 \\ 0 & A_S \end{bmatrix} \begin{bmatrix} x_C \\ x_S \end{bmatrix} + \begin{bmatrix} B_C \\ B_S \end{bmatrix} u + \begin{bmatrix} v_C \\ v_S \end{bmatrix}$$

$$[y] = \begin{bmatrix} C_C & C_S \end{bmatrix} \begin{bmatrix} x_C \\ x_S \end{bmatrix} + w$$

where x_C is the state vector to be controlled
x_S is the state vector to be suppressed
y is the measurement vector based on x_C & x_S
A_C, B_C, C_C, A_S, B_S, C_S are constant matrices
v_C, v_S, w are white Gaussian noise

10129615-97A

Figure 2-3. Design Model

$$\dot{x}_C = A_C x_C + B_C u + v$$
$$y_C = C_C x_C + w$$

where x_C is state vector to be controlled
u is control vector
y_C is measurement based on x_C
A_C, B_C, C_C are constant matrices
v, w are white, Gaussian noise

10129615-13A

Figure 2-4. Control Model

introduced by truncating states x_s and x_r. Thus our truncation problem is twofold, we must deal with the truncation of known and unknown modal states.

The basic Model Error Sensitivity Suppression (MESS) algorithm copes with the truncation of known modal characteristics by incorporating information from the design model in the optimal performance index such that the states x_s receive reduced controller excitation, (References 8-13). These known suppressed states are essentially decoupled from controller action.

However, complete solution to the LSS control problem requires some means to cope with the truncation of the unknown residual states x_r of the evaluation model. Recall that we have essentially zero knowledge concerning these modal states, except perhaps location of a lower bound in the modal frequency spectrum. Thus we adopt the roll-off filter approach and attenuate what we do not know, but with the added stipulation that the control algorithm must be capable of working through the filter.

The outline of this report is as follows:

1) We develop a filter accommodation algorithm that is compatible with optimal control and Model Error Sensitivity Suppression (MESS). Filter accommodation allows the designer to select the roll-off filter dynamics as required and develops an optimal control algorithm specific to the chosen filter dynamics. Thus Filter Accommodated Model Error Sensitivity Suppression (FAMESS) provides complete solution for the truncation of known and unknown modal coordinates.

2) A simple two-mode design model using second order filters is presented.

3) Extensions to the filter accommodation technique are briefly outlined. These include output feedback, and through duality theory Kalman filtering. Our results are preliminary on this last item.

2.2 FREQUENCY RESPONSE AND FULL STATE FEEDBACK

One of the characteristics of closed-loop systems designed by optimal control methods is high bandwidth. In many systems the optimality condition tends to undo (cancel might be more descriptive) all dynamics and rearrange parameters such that the resulting system has a flat frequency response in the controlled frequency region and rolls off as (1/s) at high frequencies. This tendency of optimal systems to be of high bandwidth is well noted in the literature, (References 14-19). This high bandwidth behavior is appropriate when system dynamics are well known, or when the physical system is relatively noise-free. Unfortunately, such conditions are rarely met in

practice. Indeed, one of the reasons that optimal regulator techniques have gained so little acceptance in the industry (Kalman filters excepted) has been the inability to translate system bandwidth requirements into adequate performance indices.

An analysis of the roll-off problem reveals that the full state feedback system, optimal or non-optimal, results in an open-loop gain matrix, $L_o(s)$, (the product of the plant and compensator matrices) which usually rolls off as (1/s). Thus, we see that as the optimal regulator belongs to the class of full state feedback systems, it usually behaves as (1/s) at high frequencies.

Thus, the solution to the roll-off problem becomes obvious: Remove the optimal regulator from the class of full state feedback systems. Hence, we develop a specific optimal control algorithm that does not require complete state feedback and is also compatible with the MESS algorithm.

It should be re-emphasized that the MESS algorithm provides solution for the problem of known modal truncation. The problem we address here is not directly amenable to these techniques as the high frequency dynamics are unknown.

Some pertinent characteristics of full state feedback systems are illustrated by the simple system of Figure 2-5. The system is of order two and we feed back two state variables, say position and velocity. Thus, the return difference which equals one plus the loop gain, $L_o(s)$, will have the structure shown. In general, as in the second order case, the numerator order of the entries $L_o(s)$ is one less than that of the denominator; these entries behave as (1/s) at high frequencies. It is this property of full state feedback systems that we seek to remove from the optimal regulator. Thus our basic approach is to find an optimal system that has gains for certain pre-selected filter states which are equal to zero. Essentially, we are seeking an optimal solution to the regulator problem that does not undo our filter dynamics. The primary property that we wish to preserve at this point is the high frequency attenuation characteristics of our filters. Hence, we resort to specific optimal control in order to preserve the desirable properties of optimal design, and simultaneously retain our control of the system bandwidth.

2.3 CONCEPTUAL BASIS FOR THE FILTER ACCOMMODATION ALGORITHM

Central to the filter accommodation algorithm is limited state feedback from a tandemly connected system. As we have seen, full state feedback results in first-order high frequency behavior. In order to achieve the roll-off desired we generate the system structure shown in Figure 2-6. The state feedback gains around the plant (states x_1) generally result in a first-order roll off. The filter is assumed to be of order f. This system transfer function matrix from r to x_2 will roll off at least as

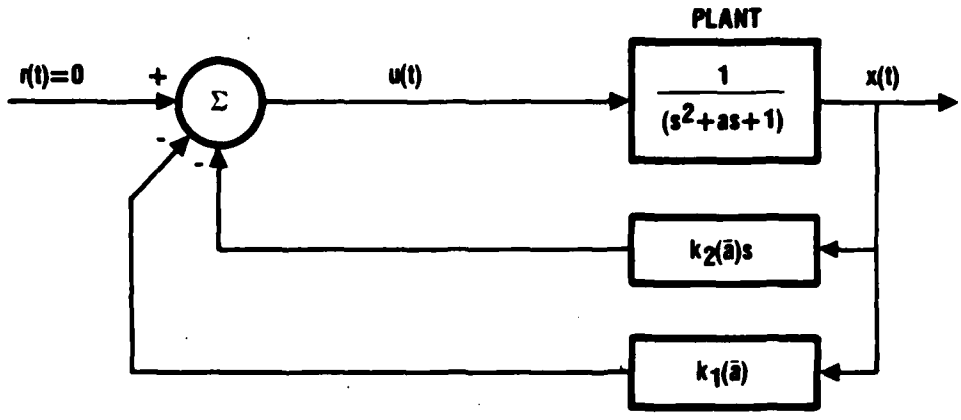

$$[1 + L_0(s)] = [1 + (k_2 s + k_1)/(s^2 + as + 1)]$$

15051275-39

Figure 2-5. Return-Difference for a Second-Order System

fast as $(1/s)^{f+1}$. Thus, the designer can specify the high frequency system behavior desired.

Now we desire the gain matrix $K = [K_1\ O]$ to be optimal. This poses a specific optimal control problem: minimize an appropriate performance index, simultaneously stabilize system I, and generate zero gains for system II.

Specific Optimal Control (S.O.C.) was developed circa 1965, pre-Luenberger Observer, to cope with the output feedback problem. The original technique ("Optimal Control with Unavailable States," John F. Cassidy, Ph.D., Thesis, R.P.I., 1969: Reference 20) was iterative in nature and required the solution of a sequence of optimal regulator problems. Sequential adjustments to the weigting matrices achieved the desired results.

The technique we develop here differs in scope and solution procedure: 1) It is not iterative, and, 2) it is not an output feedback scheme, but rather an "internal" feedback problem where states, x_1 behind the filter subsystem are fed back. Thus, in the final implementation, an estimator will be employed, but in our control law we will only feed back estimates of the substate vector x_1. If the filter states, x_2, are easily

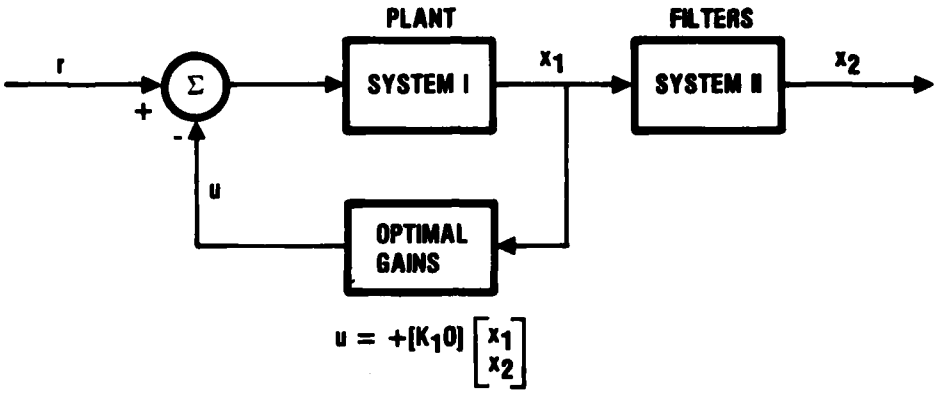

15051275-12

Figure 2-6. Conceptual Diagram for Filter Accommodation

accessible, reduced order estimation can be employed, i.e., in many situations we would not estimate the filter states. Hence, our basic approach is to develop state gain matrices of the form shown in Figure 2-6 and feed back estimates of these states as required.

As Figure 2-7 illustrates, the closed-loop system structure that results from application of the filter accommodation technique consists of the tandem connection of plant, filters, and optimal compensator. An additional feedback loop from compensator to the filtering system results from application of the algorithm. This secondary feedback path is static in nature (a matrix of constant gains) and compensates for the effect of zero feedback gains from the filter states. The filter accommodation matrix also functions as an additional input matrix for the filtering system.

2.4 OVERVIEW OF THE ALGORITHM DERIVATION

The filter accommodation algorithm is developed as follows:

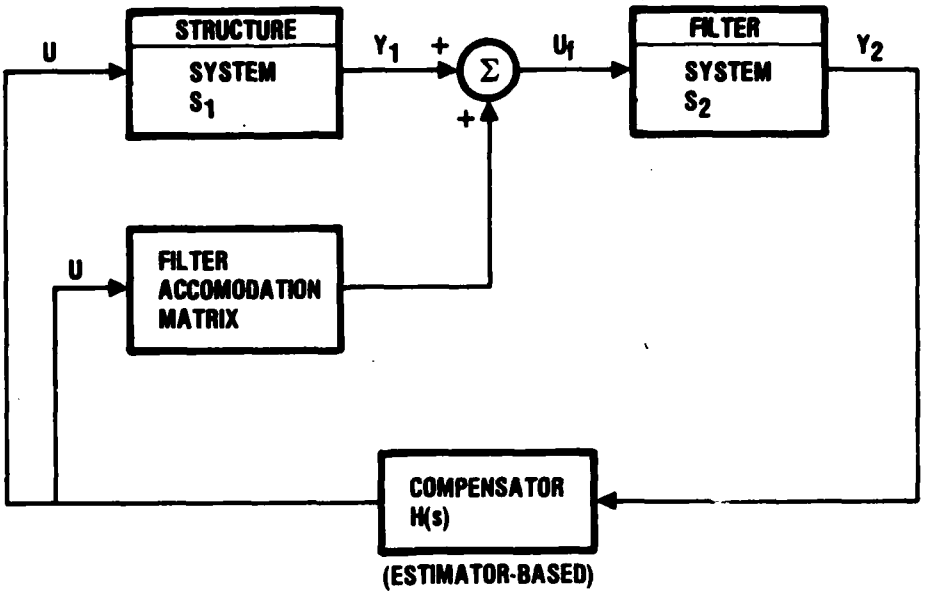

Figure 2-7. Control System Structure for Prespecified Filter Dynamics

1) Formulate the problem as that of a tandemly connected system such that a first dynamic system drives a second dynamic system, but not vice versa.

2) Form the algebraic Riccati equation for the tandem system. This allows us to observe the optimal coupling which would exist in a full state feedback optimal control solution.

3) Impose the zero gain conditions on the partitioned Riccati equation. This allows us to look for simplification and possible solution techniques.

4) Observe that after imposition of the zero gain conditions, the algebraic Riccati equation is decoupled into three subsystems that allow sequential solution: A Liapunov equation for the filter (system II); a Sylvester equation that couples the plant (system I) with the filters (system II). And a modified Riccati equation which provides stabilization for system I (the plant).

Figure 2-8 provides the detailed view of the tandem system which illustrates the notation and symbology that we shall use in our development of the filter accommodation algorithm.

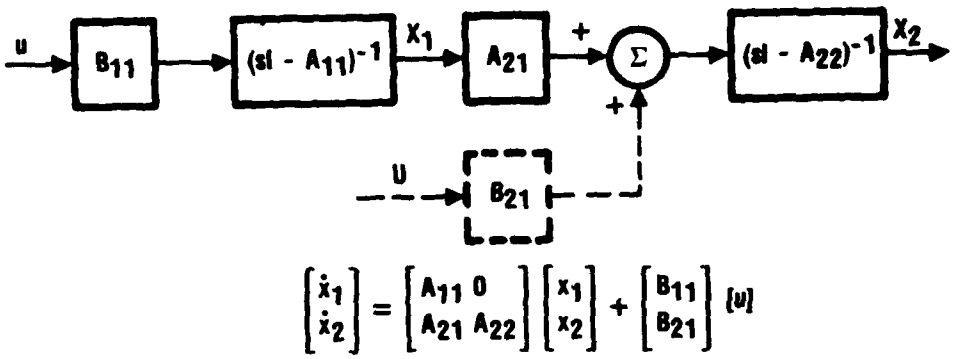

Figure 2-8. Tandem System Structure

System (A_{11}, B_{11}) corresponds to the plant and System (A_{22}) corresponds to the filters. Matrix A_{21} corresponds to the coupling between the output of the plant and the input to the filtering system. The matrix, B_{21}, indicated by the dashed lines, initially zero, is determined during the design process. The matrix B_{21} functions as an additional input matrix for the filter system. B_{21} is determined so as to force the zero-gain solution in the state regulator. The introduction of matrix B_{21} eliminates the need for iteration present in Cassidy's method.

Matrix representation of the tandem system yields the form shown in Figure 2-8. The zero submatrix in the upper right-hand corner of the A-matrix implies the tandem

connection: Matrix A_{12} is identically equal to zero; thus, system states x_1 drive system states x_2, but states x_2 do not in turn drive states x_1. The coupling is only unidirectional, as shown in the block diagram.

2.5 DERIVATION OF THE ALGORITHM

Direct substitution of the tandem equations into the algebraic Riccati equation yields the coupled algebraic equations shown in Figure 2-9. Our primary emphasis will be on the quadratic term involving R-inverse, and we will decouple these equations with an appropriate choice of the B_{21} matrix.

To simplify unwieldy algebraic expressions, we define the matrices W_{11}, W_{21}, as shown in Figure 2-10, and indicate the term by term expansion of the quadratic factors. In sequel we shall set W_{21} identically equal to zero and thus decouple our equations.

With reference to Figure 2-11, analysis of the optimal feedback gain matrix provides the constraint condition that we desire: zero feedback for states x_2. Thus, following equation (1) we partition the gain matrix into submatrices K_1 and K_2. We next apply the relationship for optimal feedback control (equations 2 and 3). Expression of the optimal control in terms of the W-matrices yields equation (4). Imposition of our constraint condition yields equation (5). Thus, we merely solve equation (5) for $B_{21}{}^T$, as shown in equation (6). In sequel we show that P_{22}-inverse always exists, thus permitting solution for B_{21}.

We note that our solution is not the only one which drives K_2 to zero. If in equation (3), B_{21} is set equal to zero, the constraint relationship becomes $B_{11}{}^T P_{12} = O$. Thus, an alternate solution would require P_{12} to lie in the kernel of $B_{11}{}^T$. At this time, it is thought that such a solution may be too restrictive; however, this null space solution is an interesting facet of the algorithm in that it would eliminate the additional feedback loop required for B_{21}. Such a development may be attractive for certain classes of control problems.

The previous development provided the motivation and conceptual overview for the filter accommodation technique. We analyzed the roll-off problem and decided full-state feedback was not desirable. We then translated the roll-off problem to a specific optimal control problem such that gains from the filter states were zero. Following this, the conditions for zero filter state gains were developed. It yet remains to be demonstrated that our constraint set yields non-conflicting solvable equations.

$$\begin{bmatrix} A_{11}^T & A_{21}^T \\ 0^T & A_{22}^T \end{bmatrix} \begin{bmatrix} P_{11} & P_{12} \\ P_{12}^T & P_{22} \end{bmatrix} + \begin{bmatrix} P_{11} & P_{12} \\ P_{12}^T & P_{22} \end{bmatrix} \begin{bmatrix} A_{11} & 0 \\ A_{21} & A_{22} \end{bmatrix} - \begin{bmatrix} P_{11} & P_{12} \\ P_{12}^T & P_{22} \end{bmatrix} \begin{bmatrix} B_{11} \\ B_{21} \end{bmatrix} [R^{-1}] [B_{11}^T \; B_{21}^T] \begin{bmatrix} P_{11} & P_{12} \\ P_{12}^T & P_{22} \end{bmatrix} = - \begin{bmatrix} Q_{11} & Q_{12} \\ Q_{12}^T & Q_{22} \end{bmatrix}$$

EXPANDING

$$\begin{bmatrix} (A_{11}^T P_{11} + A_{21}^T P_{12}^T) & (A_{11}^T P_{12} + A_{21}^T P_{22}) \\ A_{22}^T P_{12}^T & A_{22}^T P_{22} \end{bmatrix} + \begin{bmatrix} (P_{11} A_{11} + P_{12} A_{21}) & P_{12} A_{22} \\ (P_{12}^T A_{11} + P_{22} A_{21}) & P_{22} A_{22} \end{bmatrix} - \begin{bmatrix} (P_{11} B_{11} + P_{12} B_{21}) \\ (P_{12}^T B_{11} + P_{22} B_{21}) \end{bmatrix} [R^{-1}] [(B_{11}^T P_{11} + B_{21}^T P_{12}^T) (B_{11}^T P_{12} + B_{21}^T P_{22})] = - \begin{bmatrix} Q_{11} & Q_{12} \\ Q_{12}^T & Q_{22} \end{bmatrix}$$

15051275-15

Figure 2-9. Partitioned Riccati Equation

$$\begin{bmatrix} (P_{11}B_{11} + P_{12}B_{21}) \\ (P_{12}^T B_{11} + P_{22}B_{21}) \end{bmatrix} [R^{-1}] [(B_{11}^T P_{11} + B_{21}^T P_{12}^T)(B_{11}^T P_{12} + B_{21}^T P_{22})] = \begin{bmatrix} W_{11} \\ W_{21} \end{bmatrix} [R^{-1}] [W_{11}^T W_{21}^T] \quad (1)$$

OR

$$\begin{bmatrix} W_{11} \\ W_{21} \end{bmatrix} [R^{-1}] [W_{11}^T W_{21}^T] = \begin{bmatrix} W_{11}R^{-1}W_{11}^T & W_{11}R^{-1}W_{21}^T \\ W_{21}R^{-1}W_{11}^T & W_{21}R^{-1}W_{21}^T \end{bmatrix} \quad (2)$$

TERM-BY-TERM EXPANSION YIELDS

$$W_{11}R^{-1}W_{11}^T = [P_{11}B_{11} + P_{12}B_{21}] [R^{-1}] [B_{11}^T P_{11} + B_{21}^T P_{12}^T] \quad (3)$$

$$W_{21}R^{-1}W_{11}^T = [P_{12}^T B_{11} + P_{22}B_{21}] [R^{-1}] [B_{11}^T P_{11} + B_{21}^T P_{12}^T] \quad (4)$$

$$W_{11}R^{-1}W_{21}^T = [P_{11}B_{11} + P_{12}B_{21}] [R^{-1}] [B_{11}^T P_{12} + B_{21}^T P_{22}] \quad (5)$$

$$W_{21}R^{-1}W_{21}^T = [P_{12}^T B_{11} + P_{22}B_{21}] [R^{-1}] [B_{11}^T P_{12} + B_{21}^T P_{22}] \quad (6)$$

15051275-16

Figure 2-10. Expansion of the Quadratic Riccati Term

FEEDBACK CONTROL IS GIVEN BY

$$u = -[K_1 \; K_2] \begin{bmatrix} x_1 \\ x_2 \end{bmatrix} \quad (1)$$

OPTIMALITY REQUIRES

$$u = -R^{-1} [B_{11}^T \; B_{21}^T] \begin{bmatrix} P_{11} & P_{12} \\ P_{12}^T & P_{22} \end{bmatrix} \begin{bmatrix} 1 \\ x_2 \end{bmatrix} \quad (2)$$

EXPANSION YIELDS

$$u = -R^{-1} [(B_{11}^T P_{11} + B_{21}^T P_{12}^T)(B_{11}^T P_{12} + B_{21}^T P_{22})] \begin{bmatrix} x_1 \\ x_2 \end{bmatrix} \quad (3)$$

OR

$$u = -R^{-1} [W_{11}^T \; W_{21}^T] \begin{bmatrix} x_1 \\ x_2 \end{bmatrix} \quad (4)$$

IT IS DESIRED THAT $K_2 = 0$ (NO FEEDBACK FROM STATES, x_2)
THUS

$$W_{21}^T = B_{11}^T P_{12} + B_{21}^T P_{22} = 0 \quad (5)$$

OR

$$B_{21}^T = -B_{11}^T P_{12} P_{22}^{-1} \quad (6)$$

RECALL B_{21} IS FREE INITIALLY

15051275-17

Figure 2-11. Analysis of the Optimal Feedback Gain Matrix

THE GAINS SATISFY

$$[K_1 K_2] = R^{-1}[W_{11}^T W_{21}^T] \quad (1)$$

THUS $K_2 = 0$, IMPLIES $W_{21}^T = (B_{11}^T P_{12} + B_{21}^T P_{22}) = 0$ (2)

AND ALL TERMS INVOLVING W_{21} ARE EQUAL ZERO

THUS

$$W_{21} R^{-1} W_{11}^T = 0 \quad (3)$$

$$W_{11} R^{-1} W_{21}^T = 0 \quad (4)$$

$$W_{21} R^{-1} W_{21}^T = 0 \quad (5)$$

AND THE QUADRATIC TERM BECOMES

$$\begin{bmatrix} W_{11}R^{-1}W_{11}^T & W_{11}R^{-1}W_{21}^T \\ W_{21}R^{-1}W_{11}^T & W_{21}R^{-1}W_{21}^T \end{bmatrix} = \begin{bmatrix} W_{11}R^{-1}W_{11}^T & 0 \\ 0^T & 0 \end{bmatrix} \quad (6)$$

WHERE

$$W_{11}R^{-1}W_{11}^T = [P_{11}B_{11} + P_{12}B_{21}][R^{-1}][B_{11}^T P_{11} + B_{21}^T P_{12}] \quad (7)$$

15051275-18

Figure 2-12. Zero-Gain Condition and the Quadratic Riccati Term

As noted in Figure 2-12, the gain matrix is partitioned into two submatrices, K_1 and K_2, and can be expressed in terms of W_{11} and W_{21}, as shown in equation (1). The condition $K_2 = O$ implies $W_{21} = O$, and all quadratic terms involving W_{21} are zero matrices, as shown in equations (3-5). Thus the quadratic term assumes the form shown in equation (6), and the quadratic submatrix involving W_{11} can be expressed as in equation (7). The sparse nature of the quadratic matrix, equation (6), ultimately results in decoupled equations allowing sequential solution.

Figure 2-13 continues the development. The partitioned Riccati equation for the tandem system with zero gain constraints imposed, takes the form shown in equation (1). Equation (1) is concise notation for four matrix equations which we indicate symbolically as equation (11), equation (12), equation (21), and equation (22). (The notation corresponds to that of matrix analysis.) In actuality, we need only analyze three matrix equations as (12) and (21) are transposes of each other because P is a symmetric matrix.

Expansion of the four matrix equations yields the relations shown in Figure 2-14. Equation (11) is a modified Riccati equation. Equations (12) and (21) are Sylvester's

$$\begin{bmatrix} A_{11}^T P_{11} + A_{21}^T P_{12}^T) & (A_{11}^T P_{12} + A_{21}^T P_{22}) \\ A_{22}^T P_{12}^T & A_{22}^T P_{22} \end{bmatrix} + \begin{bmatrix} (P_{11} A_{11} + P_{12} A_{21}) & P_{12} A_{22} \\ (P_{12}^T A_{11} + P_{22} A_{21}) & P_{22} A_{22} \end{bmatrix}$$

$$- \left[\begin{array}{cc:c} (P_{11} B_{11} R^{-1} B_{11}^T P_{11} + P_{11} B_{11} R^{-1} B_{21}^T P_{12}^T + P_{12} B_{21} R^{-1} B_{11}^T P_{11} + P_{12} B_{21} R^{-1} B_{21}^T P_{12}^T & 0 \\ & & \\ 0^T & & 0 \end{array}\right]$$

$$+ \begin{bmatrix} Q_{11} & Q_{12} \\ Q_{12}^T & Q_{22} \end{bmatrix} = \begin{bmatrix} 0 & 0 \\ 0^T & 0 \end{bmatrix}. \qquad (1)$$

THUS WE HAVE FOUR EQUATIONS WHICH MAY BE INDICATED SYMBOLICALLY AS:

$$\begin{bmatrix} (11) & (12) \\ (21) & (22) \end{bmatrix}$$

15051275-19

Figure 2-13. The Riccati Equation with Zero-Gain Conditions Imposed

EQUATION (11) — MODIFIED RICCATI EQUATION

$$(A_{11}^T P_{11} + A^T{}_{21} P_{12}^T) + (P_{11}A_{11} + P_{12}A_{21}) - (P_{11}B_{11}R^{-1}B_{11}^T P_{11} + P_{11}B_{11}R^{-1}B_{21}^T P_{12}^T + P_{12}B_{21}R^{-1}B_{11}^T P_{11} - P_{12}B_{21}R^{-1}B_{21}^T P_{12}^T) + Q_{11} = 0 \quad (1)$$

EQUATION (12) — SYLVESTERS EQUATION

$$A_{11}^T P_{12} + P_{12}A_{22} + A_{21}^T P_{22} + Q_{12} = 0 \quad (2)$$

EQUATION (21) — SYLVESTER'S EQUATION [EQN's (12) AND (21) ARE TRANSPOSES]

$$P_{12}^T A_{11} + A_{22}^T P_{12}^T + P_{22}A_{21} + Q_{12}^T = 0^{-T} \quad (3)$$

EQUATION (22) — LIAPUNOV EQUATION

$$A_{22}^T P_{22} + P_{22}A_{22} + Q_{22} = 0 \quad (4)$$

15051275-20

Figure 2-14. Zero-Gain Riccati Subsystems

equations. Equation (22) is a Liapunov equation. Thus all matrix equations are well known, and are solvable by currently available computer algorithms (Reference 21).

We next analyze the three matrix equations from the viewpoint of sequential solvability in an overall control algorithm. The solution procedure is outlined in Figure 2-15. We first analyze the Liapunov equation.

The Liapunov equation is decoupled from the remaining equations. Recall that matrix A_{22} corresponds to the filter dynamics. As the filtering system is assumed to be stable and under the designer's control, this equation always has a solution. Thus P_{22} is a positive definite symmetric matrix, and P_{22}-inverse always exists. The weighting matrix, Q_{22} is free and can be used to condition the solution for P_{22}, i.e., increase or decrease its norm. However, the fact that Liapunov's equation is not a function of the remaining submatrices is important to our development because it permits sequential solution of the optimal control problem.

Analysis of Sylvester's equation reveals that it is a function of P_{22}, but not of any remaining, and as yet unknown, submatrices. Matrix P_{22} is known, and matrix Q_{12}

1) SOLVE THE LIAPUNOV EQUATION FOR P_{22}

$$A_{22}^T P_{22} + P_{22} A_{22} + Q_{22} = 0 \qquad (1)$$

2) SOLVE SYLVESTER'S EQUATION FOR P_{12}

$$A_{11}^T P_{12} + P_{12} A_{22} = -(Q_{12} + A_{21}^T P_{22}) \qquad (2)$$

3) SOLVE THE FILTER ACCOMMODATION EQUATION FOR B_{21}

$$B_{21} = -P_{22}^{-T} P_{12}^T B_{11} \qquad (3)$$

4) SOLVE THE MODIFIED RICCATI EQUATION FOR P_{11}

$$(A_{11}-M_{11})^T P_{11} + P_{11}(A_{11}-M_{11}) + P_{11} B_{11} R^{-1} B_{11}^T + \tilde{Q}_{11} = 0 \qquad (4)$$

WHERE

$$M_{11} = B_{11} R^{-1} B_{21}^T P_{12} \qquad (4a)$$

$$\tilde{Q}_{11} = Q_{11} + (A_{21}^T P_{12}^T + P_{12} A_{21}) - P_{12} B_{21} R^{-1} B_{21}^T P_{11} \geq 0 \qquad (4b)$$

4*) ALPHA-SHIFT TECHNIQUES CAN BE USED TO MODIFY M_{11}

15051275-21

Figure 2-15. Algorithm Solution Steps

is arbitrary; thus, we can solve Sylvester's equation for P_{12}. This equation has solution, provided A_{11} and A_{22} have no common eigenvalues. As A_{11} is generated by the plant and A_{22} is generated by the filters, this condition is easily met and imposes no severe restriction on the solution process. At this stage, enough information exists to permit calculation of B_{21}, the filter accommodation matrix, which satisfies $B_{21} = -P_{22}^{-T} P_{22}^{T} B_{11}$. We also note that the designer has a large degree of freedom in shaping B_{21}, because P_{22} and P_{12} are nearly free. An alternate solution procedure is to choose P_{22} and P_{12} such that they satisfy their respective equations and treat Q_{22} and Q_{12} as slack variables, which are determined by choice of P_{22} and P_{12}.

We can now solve the modified Riccati equation. All submatrices are known except P_{11} which is the solution of the modified Riccati equation. The Riccati equation may be simplified, as shown in equation (4), Figure 2-15.

The additional matrix M_{11}, which augments A_{11}, functions as an α-shift matrix and hence poses no problems (Reference 15). (M_{11} can also be treated as a parameter arising from a generalized performance index which involves a cross product term between the states and control vector, but we don't adopt that approach here.)

The modified state-weighting matrix $\tilde{Q}_{11}$ poses no problem as the terms comprising it are known with the exception of Q_{11} which is an arbitrary positive semi-definite matrix. Thus Q_{11} can be adjusted to ensure that $\tilde{Q}_{11}$ is a positive definite (or semi-definite matrix as required.

Hence, all equations resulting from the filter accommodation technique are solvable for the appropriate system gains, as shown in Figure 2-15.

With regard to Figure 2-15, the solution steps (1) through (4) have been discussed in detail. The additional step (4*) simply points out that if the M_{11} —matrix arising from the algorithm results in an unsatisfactory eigenvalue spectrum, α-shift techniques can be employed to readjust the closed-loop system eigenvalues.

OUR APPROACH IS EQUIVALENT TO SOLVING

$$\min_{u} J = \int_{o}^{\infty} (x^T Q x + u^T R u)\, dt \qquad (1)$$

SUBJECT TO

$$\begin{bmatrix} \dot{x}_1 \\ \dot{x}_2 \end{bmatrix} = \begin{bmatrix} A_{11} & 0 \\ A_{21} & A_{22} \end{bmatrix} \begin{bmatrix} x_1 \\ x_2 \end{bmatrix} + \begin{bmatrix} B_{11} \\ B_{21} \end{bmatrix} [u] \qquad (2)$$

WHERE THE MATRIX R IS AS BEFORE AND

$$Q = \begin{bmatrix} Q_{11} & Q_{12} \\ Q_{21}^T & Q_{22} \end{bmatrix} ; \text{ WITH } B_{21} = B_{21}(P_{12}P_{11}^{-2}) \text{ KNOWN}$$

SUCH THAT

$$u^* = -R^{-1} [(B_{11}^T P_{11} + B_{21}^T P_{12}^T) \mid 0] \begin{bmatrix} x_1 \\ x_2 \end{bmatrix} \qquad (3)$$

15051275-22

Figure 2-16. Complete Optimal Control Problem

It should be noted that the filter accommodation technique is compatible with the MESS algorithm: i.e., the MESS algorithm works through the performance index via the control weighting matrix R. The filter accommodation technique does not adjust R, but rather permits zero gain state feedback solutions via the filter accommodation matrix B_{21}.

The sequential solution of the optimal control problem just presented is equivalent to solving the standard optimal control problem illustrated in Figure 2-16. Substitution of the state weighting-submatrices used in the sequential solution, and the calculated value for the initially unknown input-matrix B_{21} will result in the specific zero gain solution shown in equation (3). However, it must be emphasized that B_{21} is unknown initially. (It can be shown that direct solution for B_{21} involves a third-order matrix equation.) The fact that our sequential solution is optimal is important because all the qualities of optimality, which do not derive from full state feedback, apply to our closed-loop system. Thus, although during the derivation and solution process we appear to have strayed from "optimality" this is not the case and we do indeed have a solution to the optimal regulator problem that requires zero feedback of the filter states. This was our original objective. The additional input matrix B_{21} for the filter states that is constructed during the process provides an additional degree of freedom such that we can obtain the required zero gains in our feedback matrix.

The final closed-loop system with estimator in place takes the form shown in Figure 2-17 where (A_p, B_p, C_p) correspond to the plant (system I of our derivation) and (A_f, B_f, C_f) correspond to the filtering system (system II of our derivation). The matrix product B_fC_p corresponds to the coupling matrix A_{21}: (with respect to our derivation: $A_p = A_{11}$, $A_f = A_{22}$, $C_p = C_{11}$, $B_p = B_{11}$, $B_m = B_{21}$, $K_p = K_1$, $x_p = x_1$, $x_f = x_2$).

The estimator is an identity optimal estimator designed via duality theory. Note that only an estimate of the controlled plant states is fed back to the plant. Also, the matrix B_m provides a minor feedback loop from the estimator output to the internal driver of the filter.

The filter/estimator system including the minor feedback loop can be thought of as a compensator attached between the plant output, y_p, located at point "a" and the plant input, u, located at point "b". As usual, our definition of the compensator is that system that has the sensor measurements as its input and the control vector as its output, i.e., the transfer function matrix between points "a" and "b" of Figure 2-17. In order to distinguish between this filter accommodated compensator, and the usual optimal compensator without the additional feedback loop through B_m, we adopt the following nomenclature: The term "compensator" will imply the usual compensator of textbook optimal control, and the term "filter-compensator" will imply a filter accommodated compensator with a filter and minor feedback loop to the filter.

After analysis of the control system structure, we may form the matrix representation of the plant-filter combination shown in Figure 2-18. The correspondence between the derivation matrices and the plant-filter matrices is indicated.

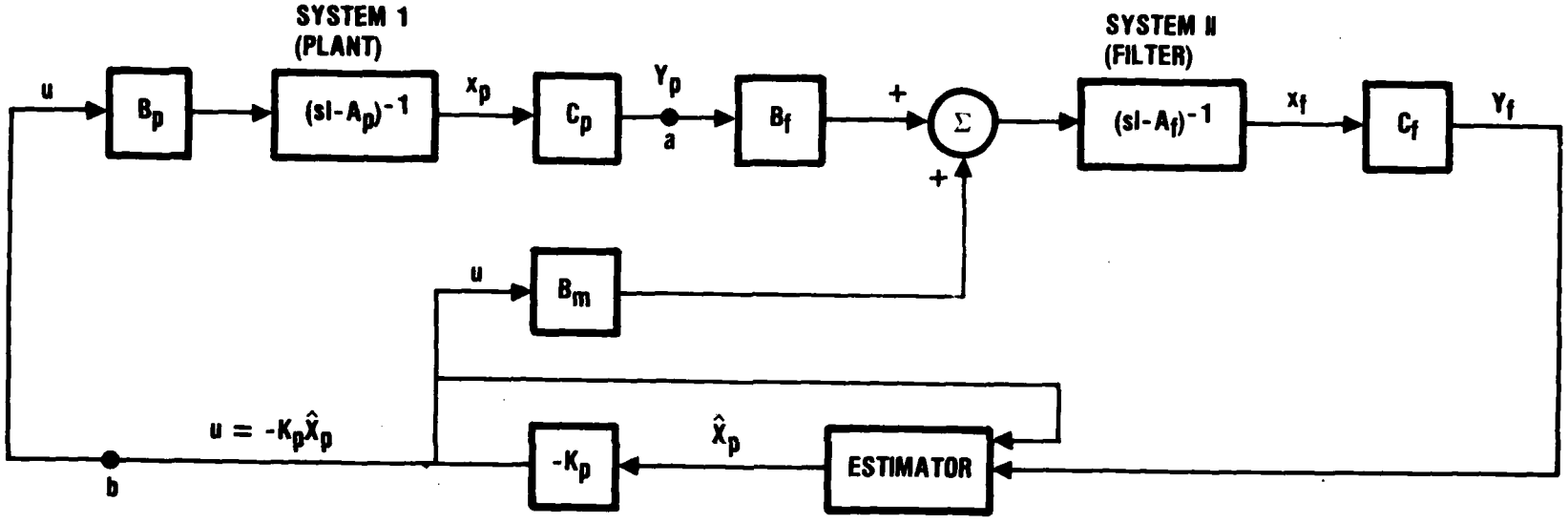

2-21

15051275-23

Figure 2-17. Detailed View of Filter Accommodated System

We held the previous notation as an analytical aid; however, during the actual design process it is more convenient to work with the new nomenclature.

THE STATE EQUATIONS FOR THE PLANT-FILTER COMBINATION

$$\begin{bmatrix} \dot{x}_p \\ \dot{x}_f \end{bmatrix} = \begin{bmatrix} A_p & 0 \\ B_f C_p & A_f \end{bmatrix} \begin{bmatrix} x_p \\ x_f \end{bmatrix} + \begin{bmatrix} B_p \\ B_m \end{bmatrix} [u] \qquad (1)$$

$$[y_f] = [0 \quad C_f] \begin{bmatrix} x_p \\ x_f \end{bmatrix} \qquad (2)$$

THUS

$$A_p = A_{11} \qquad B_p = B_{11} \qquad C_f = C_{12}$$
$$A_f = A_{22} \qquad B_m = B_{21} \qquad x_p = x_1$$
$$B_f C_p = A_{21} \qquad C_p = C_{11} \qquad x_f = x_2$$

15051275-24

Figure 2-18. Plant-Filter Equations

2.6 DESIGN EXAMPLE

These design examples illustrate the effectiveness of the filter accommodation algorithm to cope with residual modes. To keep the examples simple we include one mode from each class: controlled, suppressed, and residual. In order to guarantee residual mode excitation we make the residual model have slopes identical to that of the controlled mode. Thus we ensure that attenuation of the residual modal response results from the filter action and not judicious actuator or sensor placement. In order that the example demonstrates the compatibility of the filter accommodation technique and the standard MESS algorithm, we also include a suppressed mode. The effectiveness of the filter accommodation technique in promoting residual mode stability is also judged by comparison with a MESS design that does not employ filter accommodation. This last step ensures that we have not worked with a benign

problem. Eigenvalue analyses are employed to judge the efficiency of the two designs. The residual modes should migrate less with the filter accommodation. Time history plots are also used to observe signals in the closed-loop system. Less high frequency noise should exist in the filter accommodated designs. These ground rules are severe - especially the equal slope condition; however, the numerical results of such a design problem should provide a clear indication of the potential of the filter accommodation algorithm.

$$\begin{bmatrix} \dot{x}_1 \\ \dot{x}_2 \\ \dot{x}_3 \\ \dot{x}_4 \end{bmatrix} = \left[\begin{array}{cc:cc} 0 & 1 & 0 & 0 \\ -1 & 0 & 0 & 0 \\ \hdashline 0 & 0 & 0 & 0 \\ 0 & 0 & -4 & 0 \end{array}\right] \begin{bmatrix} x_1 \\ x_2 \\ x_3 \\ x_4 \end{bmatrix} + \left[\begin{array}{cc} 0 & 0 \\ 0.259 & 0.966 \\ \hdashline 0 & 0 \\ 1.73 & 1.00 \end{array}\right] \begin{bmatrix} u_1 \\ u_2 \end{bmatrix} \qquad (1)$$

$$\begin{bmatrix} y_1 \\ y_2 \end{bmatrix} = \begin{bmatrix} 0 & 0.259 & 0 & 1.73 \\ 0 & 0.966 & 0 & 1.0 \end{bmatrix} \begin{bmatrix} x_1 \\ x_2 \\ x_3 \\ x_4 \end{bmatrix} \qquad (2)$$

WHERE

$$x_c \equiv \begin{bmatrix} x_1 \\ x_2 \end{bmatrix} \text{ AND } x_2 \equiv \begin{bmatrix} x_3 \\ x_4 \end{bmatrix} \qquad (3)$$

ONE PERCENT DAMPING ADDED TO THE MODES

15051275-38

Figure 2-19. Example Design Model

As shown in Figure 2-19, a two-mode design model is employed. This model has frequencies at one and two radians. We choose to control the one radian mode and suppress control action to the two radian mode. Thus the controlled state vector is composed of states x_1 and x_2, and the suppressed state vector is composed of states x_3 and x_4. The actuators and sensors are colocated therefore $B = C^T$.

The input matrices have the directions shown in Figure 2-20. ($B_c = b_2 = B_r$ same residual and controlled mode slopes.) Thus, $B_cK = B_rK$ and the control action applied to the residual and controlled modes is identical. The residual modes will most certainly be excited and thus we will be able to check the efficiency of the filters in reducing observation spillover.

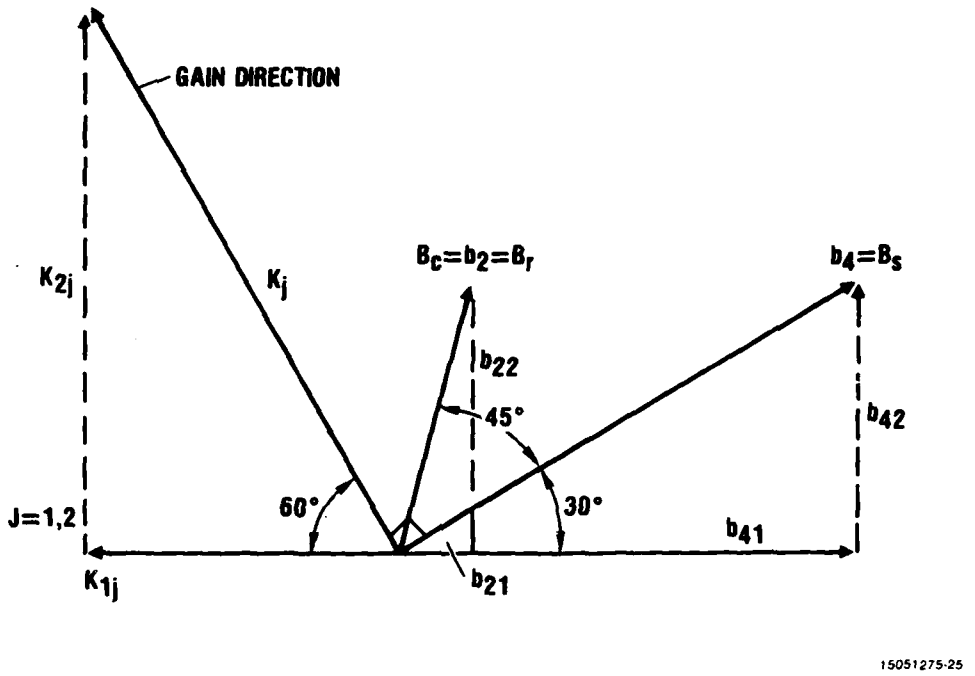

Figure 2-20. Modal Input Matrix Row-Vector Directions

One aspect of filter accommodation is the ability to provide attenuation which starts deep within the controlled region and still provide the proper amount of control authority to meet performance requirements. To demonstrate this aspect of the algorithm we choose a second-order filter that corners at one-tenth of a radian. The controlled mode at one radian is a decade away from the filter corner frequency and thus experiences, when viewed from the filter, over 40 decibels of attenuation. Figure 2-21 illustrates the filter frequency response.

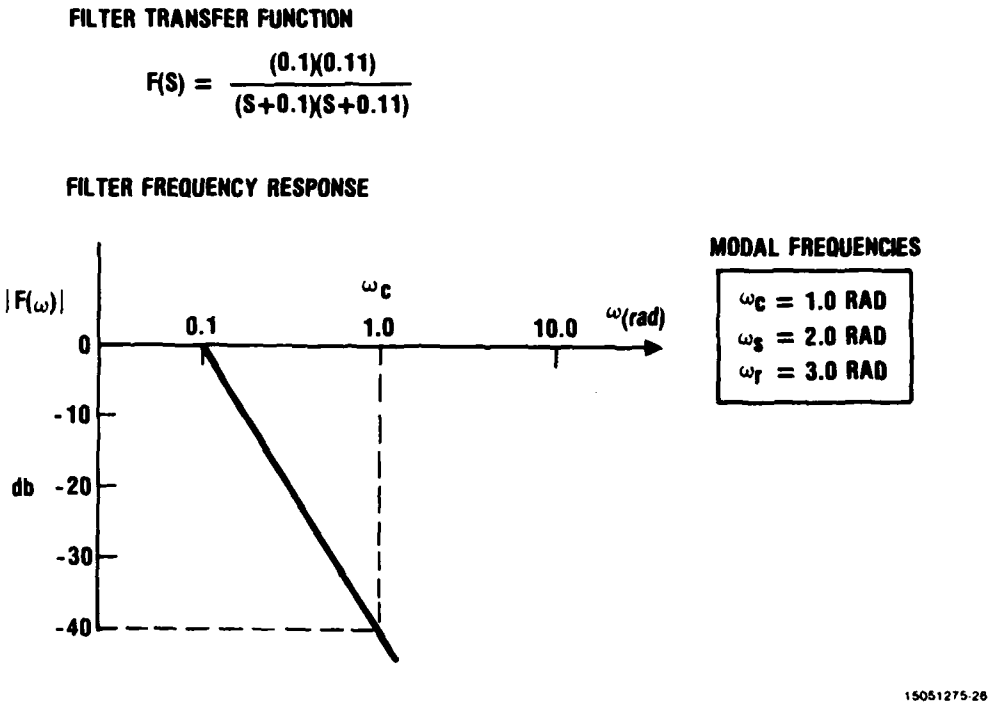

Figure 2-21. Roll-Off Filter Characteristics

2.6.1 TIME HISTORIES. We next apply a unit initial condition to Mode 1 and examine the transient response of all signals around the loop. Figure 2-22 illustrates the response of modal positions: Mode 1, the controlled mode, behaves quite well and exhibits the required damping characteristics, Mode 2, the suppressed mode, receives a small amount of excitation ($\approx 10^{-11}$) and behaves in open loop fashion. Mode 3, the residual mode is excited by controller action ($\approx 10^{-1}$) and rings in open-loop fashion.

Figure 2-23 illustrates the sensor and filter responses. The excited residual mode spills out into the sensors and the filter effectively attenuates the residual mode response.

2.6.2 COMPARISON WITH A NONFILTER ACCOMMODATED DESIGN. To check the efficiency of filter accommodation to cope with residual mode spillover, a non-filter accommodated design employing the standard MESS algorithm is applied to the design model. The design parameters (a-shift and suppression level) are identical for

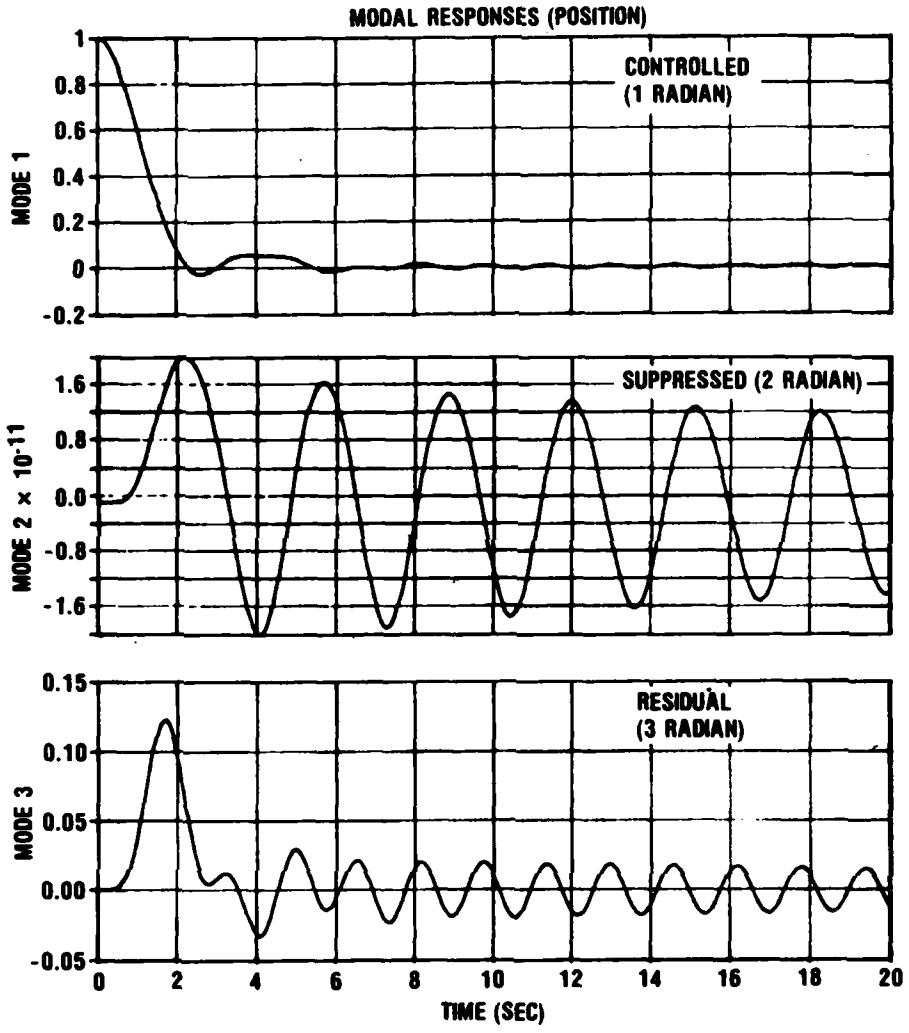

15051275-27

Figure 2-22 Modal Response (Position)

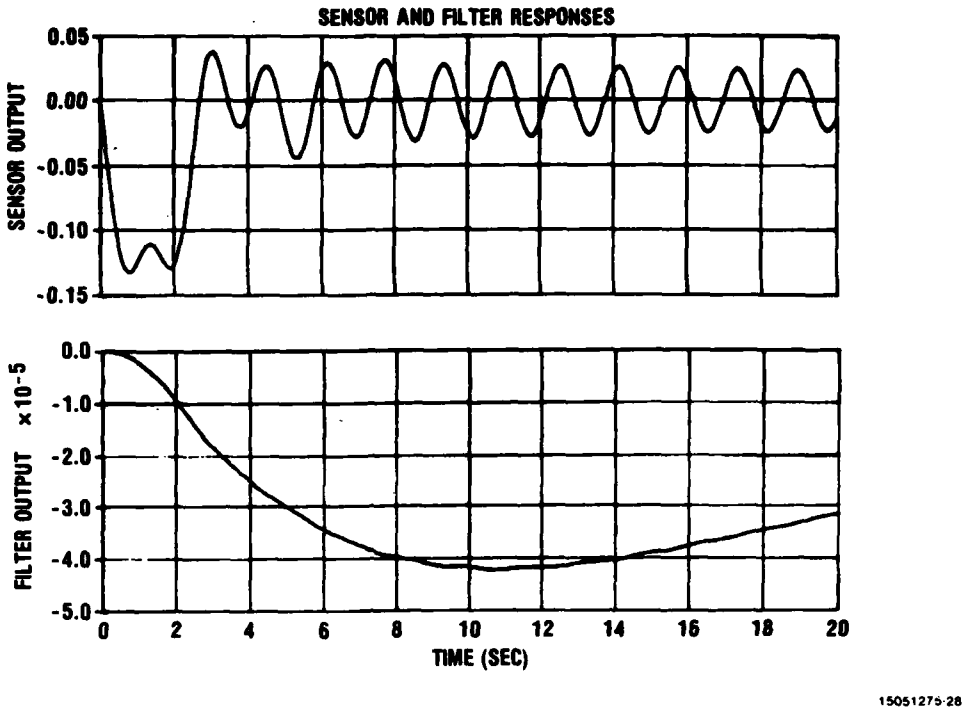

Figure 2-23. Sensor and Filter Responses

both designs. Eigenvalue data for the designs is presented in Tables 2-1 and 2-2. Due to observation spillover the nonfilter accommodated design is unstable. Instability occurs with the associated residual mode eigenvalues of $1.4 \pm j\ 4.9$. The corresponding residual mode eigenvalues for the filter accommodated design are $-2.2 \times 10^{-2} \pm j\ 3.9$, which indicates a small shift in the real part of the closed-loop root from its open loop value of -2.0×10^{-2}. Thus, the comparison indicates that the evaluation model was not benign and demonstrates the efficiency of the design algorithm relative to this example. Figure 2-24 depicts the residual mode root migration of the two designs vectorially.

2.6.3 FREQUENCY RESPONSE ANALYSIS. The filter accommodation algorithm was developed to provide bandwidth control for the LQG design process. With respect to large space system control, this implies that all modes above a certain frequency spectrum are gain stabilized. To demonstrate the effectiveness of the algorithm, we compare the frequency response of the open-loop gain matrix $L_o(s)$ for our two design

Table 2-1. Nonfilter-Accommodated Eigenvalues (Unstable)

Eigen No.	Real Part	Imaginary Part	Resultant Value	Angle (degrees)	Damping Ratio	
1	−13.72	0.	13.72	180.0	1.000	
2	1.403	4.903	5.100	74.03	−.2751	Residual
3	1.403	−4.903	5.100	−74.03	−.2751	
4	−1.9645	0.	.9645	180.0	1.000	
5	−.4258	1.731	1.783	103.8	.2388	
6	−.4258	1.731	1.783	−103.8	.2388	
7	−2.0000E-02	2.000	2.000	90.57	1.0000E-02	Suppressed
8	−2.0000E-02	−2.000	2.000	−90.57	1.0000E-02	

15051275-10

Table 2-2. Filter Accommodated Eigenvalues (Stable)

Eigen No.	Real Part	Imaginary Part	Resultant Value	Angle (degrees)	Damping Ratio	
1	−5.547	3.421	6.518	148.3	.8511	
2	−5.547	−3.421	6.518	-148.3	.8511	
3	−5.962	0.	5.962	180.0	1.000	
4	−2.3242E-02	3.917	3.917	90.34	5.9333E-03	Residual
5	−2.3242E-02	−3.917	3.917	−90.34	5.9333E-03	
6	−.5654	1.723	1.813	108.2	.3119	
7	−.5654	−1.723	1.813	−108.2	.3119	
8	−.1000	0.	.1000	180.0	1.000	
9	−.1100	0.	.1100	180.0	1.000	
10	−.8789	0.	.8789	180.0	1.000	
11	−3.227	.7342	3.309	167.2	.9751	
12	−3.227	−.7342	3.309	−167.2	.9751	
13	−2.0000E-02	2.000	2.000	90.57	1.0000E-02	Suppressed
14	−2.0000E-02	−2.000	2.000	−90.57	1.0000E-02	
15	−.1100	0.	.1100	180.0	1.000	
16	−1.0000E-01	0.	1.0000E-01	180.0	1.000	

15051275-9

examples. This comparison is made for plants with and without residual modes. Also the frequency response of the optimal compensators are compared for each design.

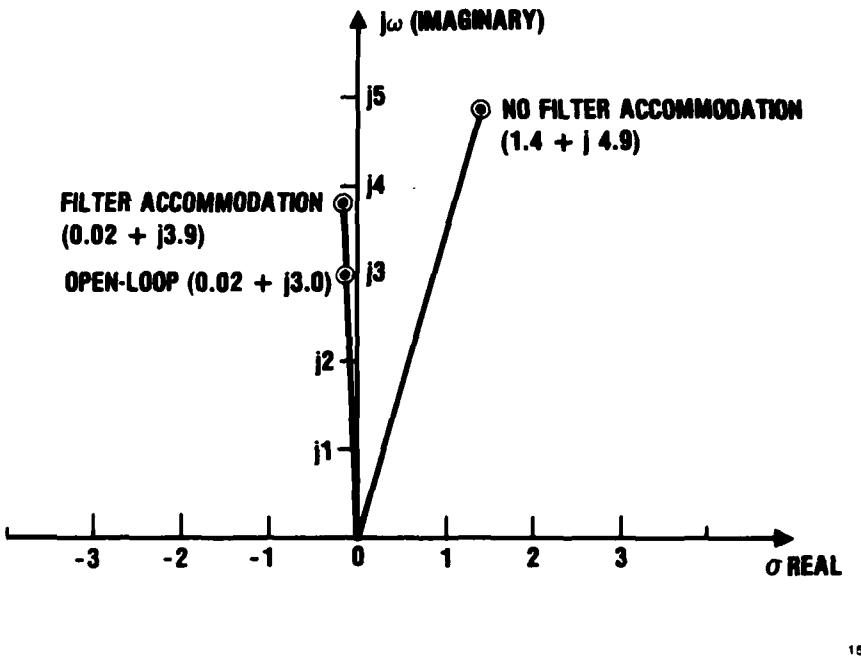

Figure 2-24. Residual Mode Root Migration

As both $L_O(s)$ and the compensator transfer characteristics are characterized by (4×4) matrices, for conciseness of presentation we provide the frequency response for the one-one entry in each case. (The remaining matrix entries exhibit similar behavior.) To determine $L_O(s)$ we break the feedback loop at point b of Figure 2-17, excite the system at actuator port number one and measure the signal returning to actuator one from the compensator. This procedure is analogous to determination of the return difference for scalar systems. In similar fashion we obtain the compensator frequency response by breaking the feedback loop at both points a and b of Figure 2-17, inject a signal at sensor port number one and observe the output signal that would be applied to actuator one. Thus we obtain the frequency response of the one-one entry of the compensator matrix.

Figure 2-25 depicts the frequency response of the one-one entry of $L_o(s)$ for the filter accommodated design. The design model of the plant (one controlled mode, one suppressed mode, and no residual modes) is employed in the frequency response generation. Examination of the plot reveals fourth-order behavior at high frequencies, i.e., 80 db roll-off/decade. This high frequency behavior can be explained as follows: the optimal controller behaves as 1/s, the optimal estimator behaves as 1/s, and the filters behave as $1/s^2$ where s is the complex Laplace transform parameter. Thus we achieve fourth-order high frequency behavior as our design analysis predicted. This fourth-order response is in contrast to the standard optimal control algorithm which provides only a second-order roll-off at high frequencies.

Figure 2-26 depicts the frequency response of the one-one entry of $L_o(s)$ for the standard optimal design. Again we employ the design model of the plant (no residual modes) for the frequency response generation. As anticipated, the plot exhibits second-order behavior at high frequencies, i.e., 40 db roll-off/decade, which corresponds to single integration behavior for both the controller and the estimator. We also note the flatness of the response curve after the resonant peak in Figure 2-26. This response is characteristic of standard optimal control designs which tend to be high bandwidth in nature. The "plateau" effect has been reduced in the filter accommodated designs.

The resonant peaks at 0.159 Hz present in both Figures 2-25 and 2-26 correspond to controlled mode resonance. The suppressed mode (0.318 Hz) is not visible in the frequency response plots. This phenomena occurs because the basic MESS optimal control algorithm employed in both designs renders the suppressed mode uncontrollable and unobservable; thus effectively blocking excitation of, and transmission from, the suppressed mode.

Additional response plots of $L_o(s)$ with residual modes included are shown in Figure 2-27 and Figure 2-28, for the filter accommodated design and the standard optimal design, respectively. Examination of the residual mode resonant peaks at 0.477 Hz reveals the attenuation effects of the filter. The resonant peak corresponding to the residual mode exhibits a magnitude of 3.5 for no filter accommodation and a magnitude of 1.2 for the filter accommodated design; a difference of approximately 8.6 db. Thus our filter accommodated design successfully attenuates the residual mode response as required.

We next examine the frequency response of the optimal compensator. The compensator is defined as that system which has the sensor vector as its input and the control vector as its output; i.e., the transfer function matrix between points "a" and "b" of

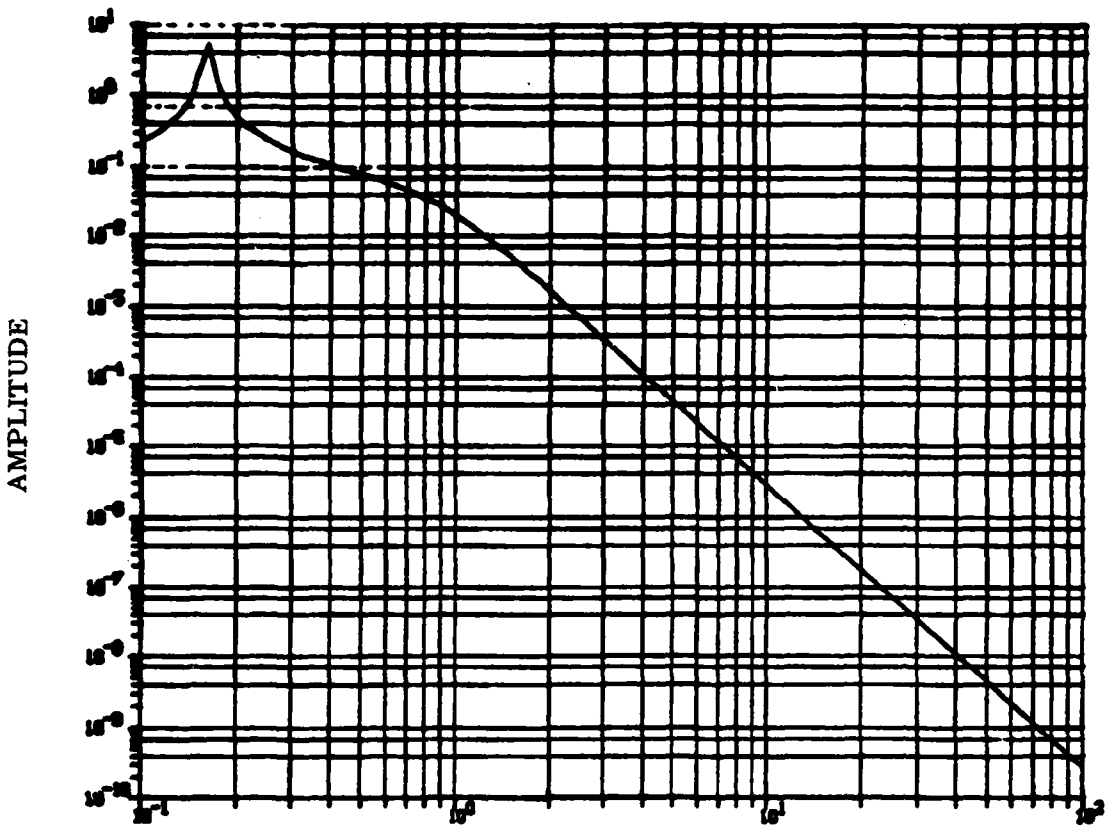

Figure 2-25. Filter Accommodated Design. Loop Gain Frequency Response for $L_O(s)$. (No Residual Modes - Design Model)

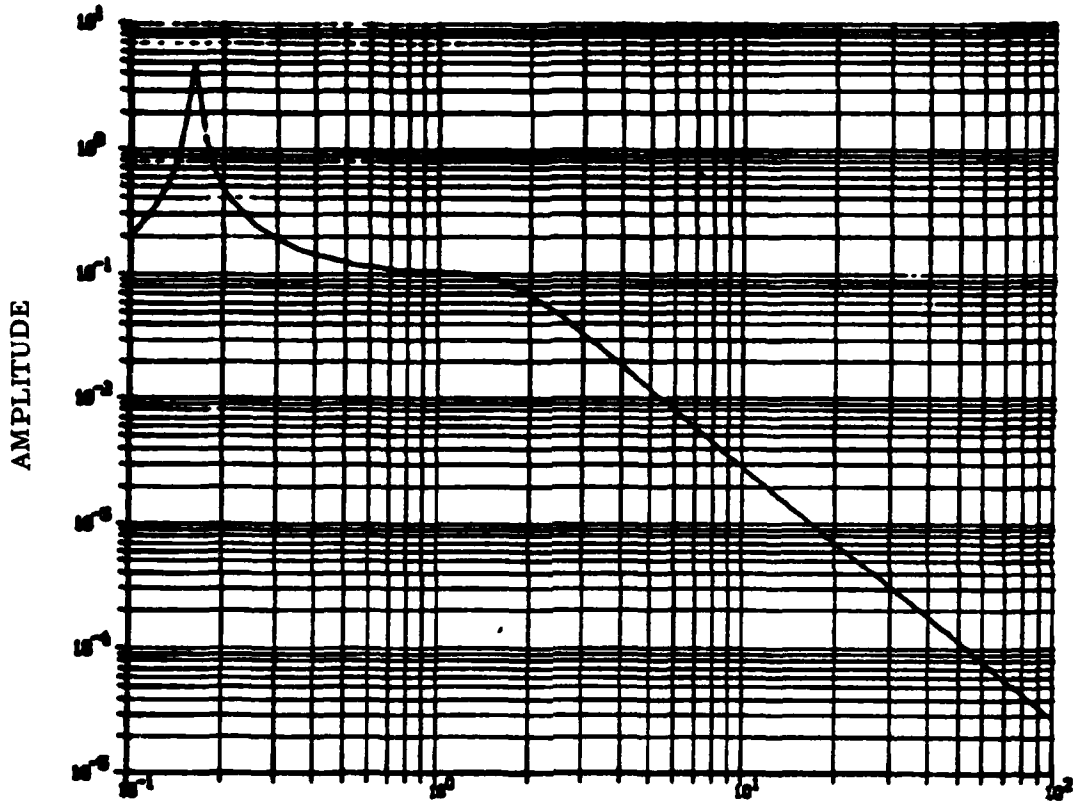

Figure 2-26. Non-Filter Accommodated Design. Loop Gain Frequency Response for $L_o(s)$. (No Residual Modes - Design Model)

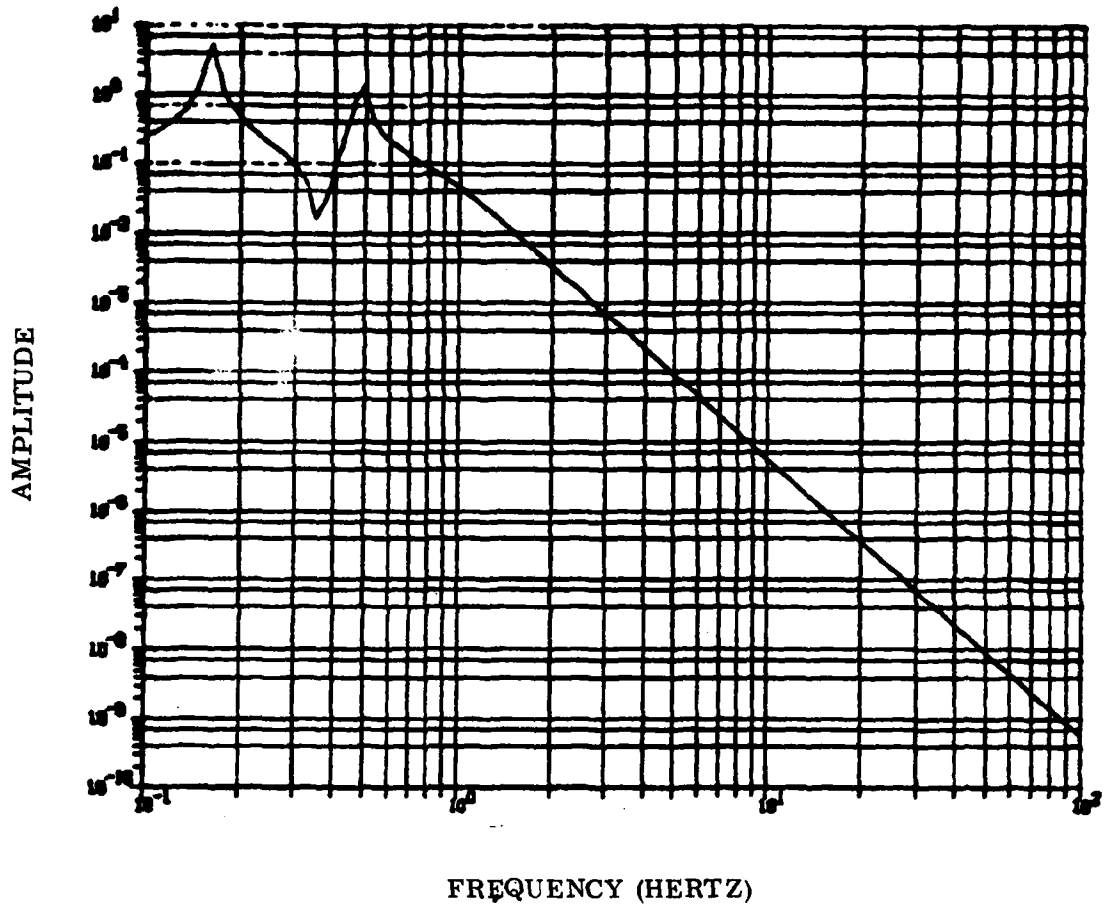

Figure 2-27. Filter Accommodated Design. Loop Gain Frequency Response for $L_o(s)$. (Residual Mode Included - Evaluation Model)

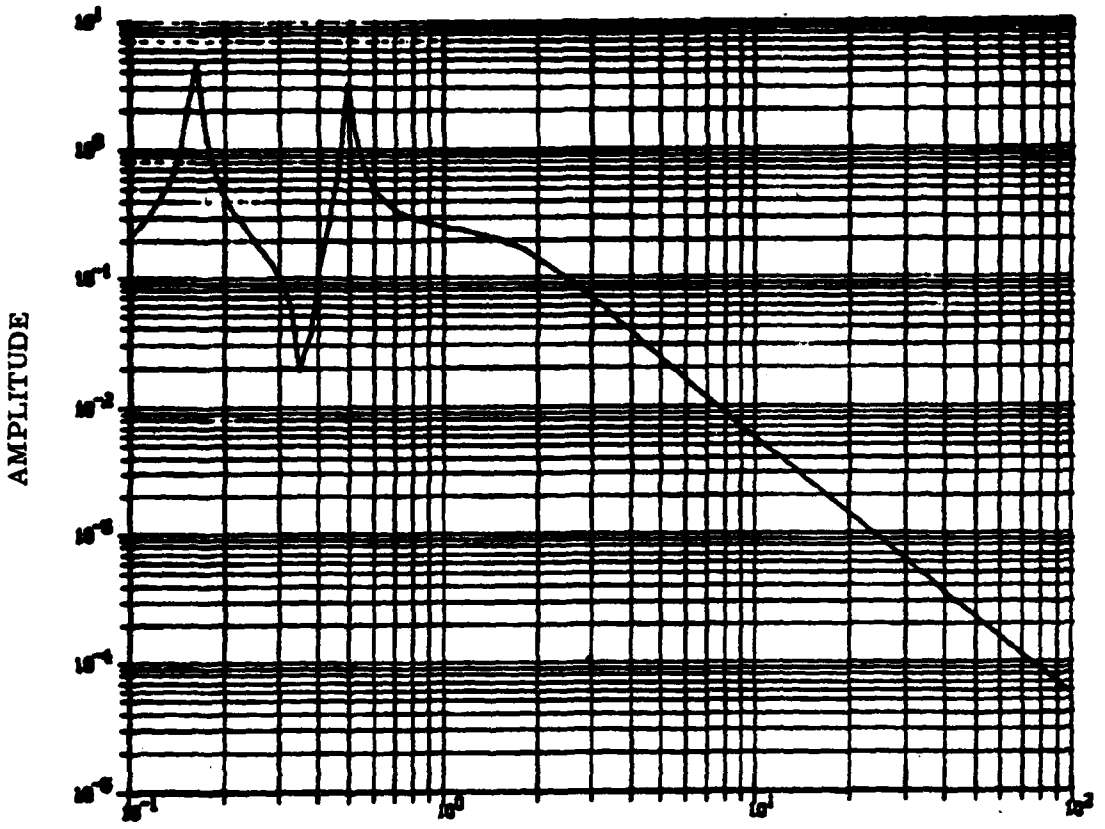

Figure 2-28. Non-Filter Accommodated Design. Loop Gain Frequency Response for $L_o(s)$. (Residual Mode Included - Evaluation Model)

Figure 2-17 for filter accommodated design. For the non-filter accommodated design, the compensator is defined precisely as before except the filters are replaced by dynamicless identity matrices and the filter accommodation matrix is a zero matrix. Figure 2-29 depicts the standard textbook optimal compensator.

Figure 2-30 displays the frequency response of the one-one entry for the filter accommodated compensator. The magnitude of the response initially remains flat (magnitude = 0.6) and then rolls off at 60 db/decade; i.e., third-order high frequency

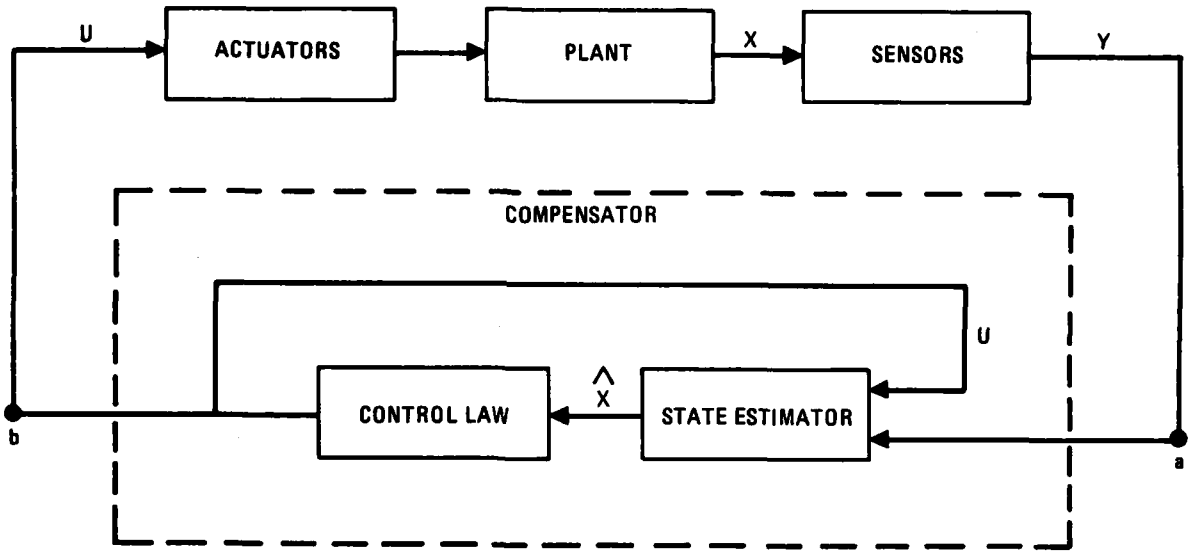

Figure 2-29. Standard Textbook Optimal Compensator

behavior. This behavior is to be expected as the filters behave as $1/s^2$ at high frequencies and estimator behaves as $1/s$. Thus the compensator behavior and the $L_o(s)$ behavior are in agreement. The additional matrix entries for the compensator response, now shown here, provide similar high frequency behavior.

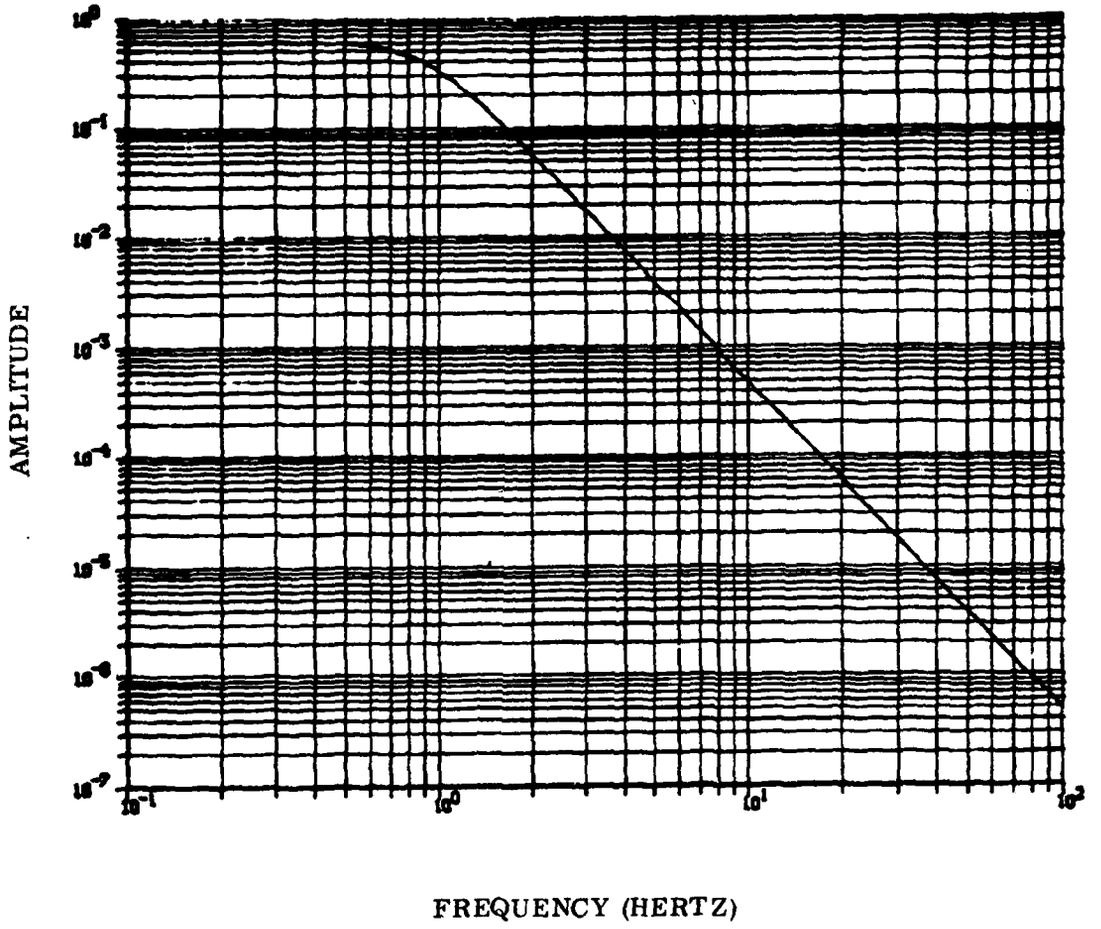

Figure 2-30. Filter Accommodated Compensator Frequency Response

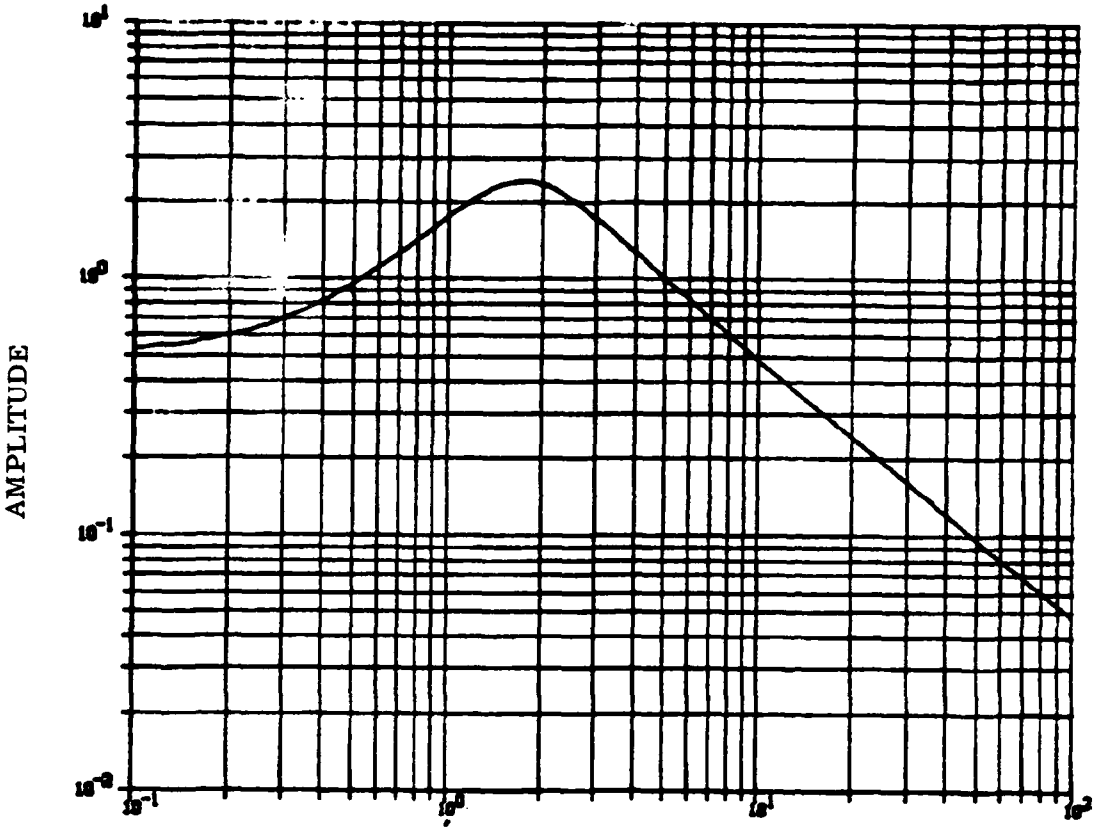

Figure 2-31. Non-Filter Accommodated Compensator Frequency Response

Figure 2-31 displays the frequency response of the one-one entry for the standard optimal compensator. This response exhibits a peak at 1.7 Hz and their rolls off at 20 db/decade; i.e., first-order behavior at high frequencies. Again this high frequency behavior is expected for the standard optimal compensator. With respect to the residual mode, the peak at 1.7 Hz represents phase lead, and is detrimental to residual mode stability; i.e., the system gain increases from approximately 0.5 to 2.5, or 14 db. This behavior also contributes to the flatness of the frequency response plot for $L_o(s)$ observed previously in Figure 2-26.

Thus the frequency response plots confirm the efficiency of our analytical design methodology and the filter accommodation algorithm provides a-priori high frequency behavior as predicted.

2.7 FILTER ACCOMMODATION AND LIAPUNOV STABILITY

The effects of the roll-off filter may be easily incorporated into a Liapunov stability analysis. The plant transfer function matrix has the form shown in equation (2) of Figure 2-32. The diagonal nature of the matrix structure results from the normal mode representation of the structure. If we perform the matrix multiplication indicated in equation (2), we obtain the linear sums shown in equations (4) and (5). Thus, the overall plant may be viewed as a linear sum of the controlled, suppressed and residual plants.

$$P(s)=C(sI-A)^{-1}B \tag{1}$$

$$P(s)=[C_C C_S C_r]\begin{bmatrix}(sI-A_C)^{-1} & 0 & 0\\ 0 & (sI-A_S)^{-1} & 0\\ 0 & 0 & (sI-A_r)^{-1}\end{bmatrix}\begin{bmatrix}B_C\\ B_S\\ B_r\end{bmatrix} \tag{2}$$

$$P(s)=C_C(sI-A_C)^{-1}B_C+C_S(sI-A_S)^{-1}B_S+C_r(sI-A_r)^{-1}B_r \tag{3}$$

$$P(s)=P_C(s)+P_S(s)+P_r(s) \tag{4}$$

Attenuate $P_r(s)$ with a filter such that $\gamma^2 << 1$

$$\gamma^2 P_r(s)=\gamma^2 C_r(sI-A_r)^{-1}B_r \tag{5}$$

The matrix C_r has been reduced by the attenuation factor:
$C_r \rightarrow \gamma^2 C_r$;

15051275-6

Figure 2-32. Roll-Off Filter Attenuation and the Open-Loop Plant Transfer Matrix

Thus, if we assume that for the residual mode frequency range the filter has an attenuation factor γ^2, this factor may be directly incorporated into the residual plant transfer function matrix, as shown.

From this perspective, the filter modifies the effective value of the input and output matrices by multiplication with a constant, i.e., $C_r \rightarrow \gamma^2 C_r$. Thus we may incorporate modified matrix in a Liapunov analysis for stability. This analysis reflects the fact that the filter attenuates observation spillover, but does not affect control spillover.

A closed-loop stability analysis for the closed-loop system involves the closed-loop system matrix shown in Figure 2-33 where it is assumed that we have an estimator in the loop: i.e., x_c, e_c, x_s, and x_r represent the controlled state vector, the error vector for the estimated controlled states, the suppressed state vector, and the residual state vector, respectively. A Liapunov analysis can be applied to this matrix.

$$\begin{bmatrix} \dot{x}_c \\ \dot{e}_c \\ \dot{x}_s \\ \hline \dot{x}_r \end{bmatrix} = \left[\begin{array}{ccc:c} A_c - B_c K & B_c K & O & O \\ O & A_c - G C_c & -G C_s & -\gamma^2 G C_r \\ -B_s K & B_s K & A_s & O \\ \hdashline -B_r K & B_r K & O & A_r \end{array}\right] \begin{bmatrix} x_c \\ e_c \\ x_s \\ \hline x_r \end{bmatrix}$$

15051275-4

Figure 2-33. Complete Closed-Loop System Matrix Including Residual Modes and Attenuation Factor

The closed-loop system matrix may be diagrammed as shown in Figure 2-34. The effect of the filter is to attenuate the response generated by the residual modes. For zero attenuation factor, the residual mode loop would be completely open. As previously noted, the residual modes are excited; control spillover is not attenuated, but observation spillover is attenuated by the filter attenuator factor. It is the attenuation of observation spillover that counteracts the potentially destabilizing effect of residual mode excitation. This unidirectional decoupling achieved by filter accommodation is not as strong as that achieved by the basic MESS algorithm; however, the MESS algorithm relies on knowledge of the decoupled modes. In the face of incomplete knowledge, except perhaps a frequency range, filter attenuation of the unknown modal responses is the best that can be achieved with linear techniques.

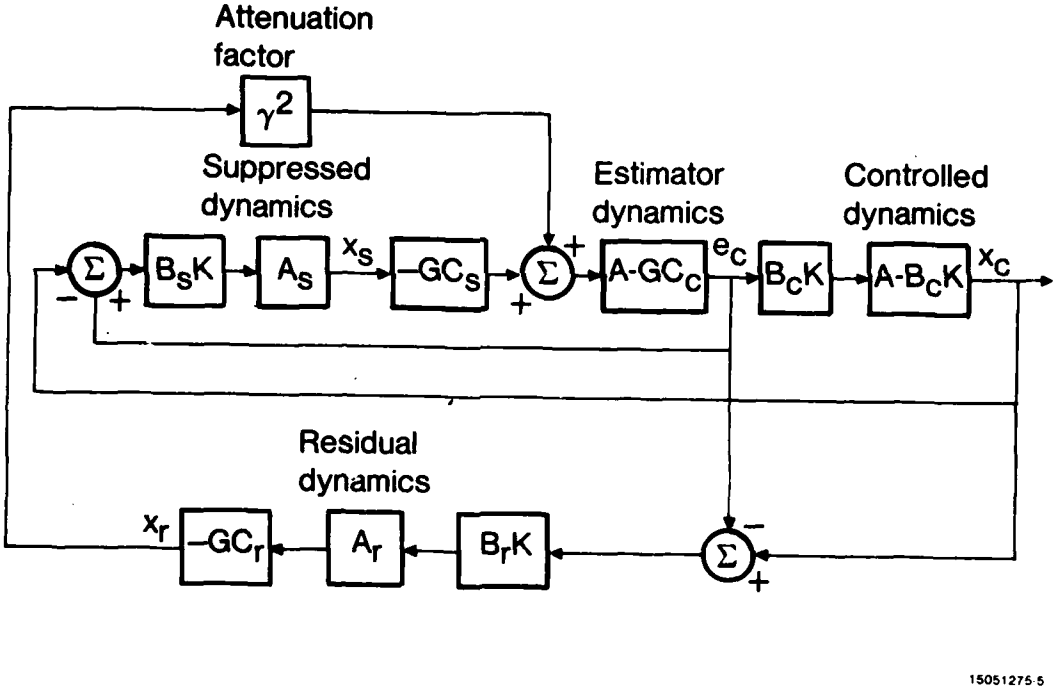

Figure 2-34. Closed-Loop System Dynamics with Residual Modes

Following Siljak's (Reference 22) decentralized Liapunov methodology we arrive at the stability conditions indicated in Figure 2-35. The Liapunov stability parameters,

the epsilons, are direct functions of the attenuation factor gamma. Thus, a conservative requirement for the degree of attenuation required by the roll-off filter is established.

The control spillover term ϵ_{21} can be expressed in standard matrix norm notation, as shown in Figure 2-36. The Schwarz inequality is then easily applied to the matrix product $B_r K$. This allows separation of the norms for both matrices. Similar results hold for observation spillover. Thus, the bounds may be expressed as shown by inequality (5). Assumptions concerning the structural damping and modal slopes together with gain levels allows calculation of the filter attenuation constant, gamma.

The expressions developed for the stability analysis provide an analytical basis for several heuristic concepts: Examination of inequality (5) reveals:

$$\frac{(\zeta_s \omega_s)(\zeta_r \omega_r)}{q_{12} q_{21}} > \epsilon_{12} \epsilon_{21}$$

where

$\zeta_s \omega_s$ = suppressed damping (min value)

$\zeta_r \omega_r$ = residual mode damping (min value)

ϵ_{12} = observer spillover term

$= \lambda_m^{1/2} (\gamma^2 C_r^T G_r^T G C_r) = \gamma \| G C_r \|$

ϵ_{21} = control spillover term

$= \lambda_m^{1/2} [2(B_r K)^T B_r K] = \sqrt{2} \| B_r K \|$

$q_{12}\, q_{12}$ = Liapunov parameters (always positive)

λ_m = Maximum eigenvalue

15051275-7

Figure 2-35. Roll-Off Filter Attenuation and Liapunov Stability

Control spillover

$$\epsilon_{21} = \lambda_m^{1/2} (2K^T B_r^T B_r K)$$
$$\leq \sqrt{2} \parallel B_r \parallel \bullet \parallel K \parallel$$

Observation spillover

$$\epsilon_{12} = \lambda_m^{1/2} (\gamma^2 C_r^T G^T G C_r)$$
$$\leq \gamma \parallel C_r \parallel \bullet \parallel G \parallel$$

thus for stability (sufficiency)

$$\frac{(\zeta_s \omega_s)(\zeta_r \omega_r)}{q_{12} q_{21}} > \parallel K \parallel \bullet \parallel G \parallel \bullet \parallel B_r \parallel \bullet \parallel C_r \parallel \bullet \sqrt{2}\, \gamma$$

15051275-8

Figure 2-36. Spillover Bounds as a Function of System Parameters

1) It is always possible to provide gain stabilization for the system, i.e., as gamma tends to zero, open-loop conditions prevail in the LSS which is open-loop stable.

2) High gain levels in both filter or estimator require heavy filtering (or a large amount of intrinsic modal damping) ensure stability. For a fixed amount of modal damping and a high gain system, the attenuation provided by the filter must be correspondingly larger to ensure satisfaction of the stability inequality.

3) The norms $\parallel K \parallel$ and $\parallel G \parallel$ are proportional to available actuator and sensor power. Thus, one can obtain stability bounds as functions of assumed residual mode damping and residual mode slope.

2.8 DISTURBANCE ACCOMMODATION

For those systems in which modal damping of itself is insufficient to meet line of sight specifications, and the Draper evaluation modal #2 falls into this class of structure, some additional control technique must be employed to meet performance criteria. Disturbance accommodation is one technique that can be employed to counteract disturbances. We choose disturbance accommodation because it allows us to integrate both open-loop and closed-loop control techniques, i.e., we can set the disturbance accommodation loop independently of the damping augmentation loop.

Disturbance accommodation falls basic into two broad classes: input disturbance estimation (E. J. Davison, Reference 23) and output disturbance estimation (C. D. Johnson, References 24 and 25). The main distinction lies in the site of disturbance sensing. One technique (input estimation) measures the disturbance at the disturbance site and leads to open-loop correction. The other technique (output estimation) measures the effect of the disturbance at the system output and leads to closed-loop correction. For large distributed systems, input estimation is preferred due to the long propagation time of the system, i.e., the disturbance could be operational for long periods of time before it was sensed at the system outputs. In addition, the open-loop correction will provide no stability problems in the face of large parameter variations. Figure 2-37 illustrates the two concepts. The disturbance canceling equation may be easily derived as follows: First we note that disturbance signal u_d must cancel the disturbance effects for any w_d. Thus we form the equations shown in Figure 2-38.

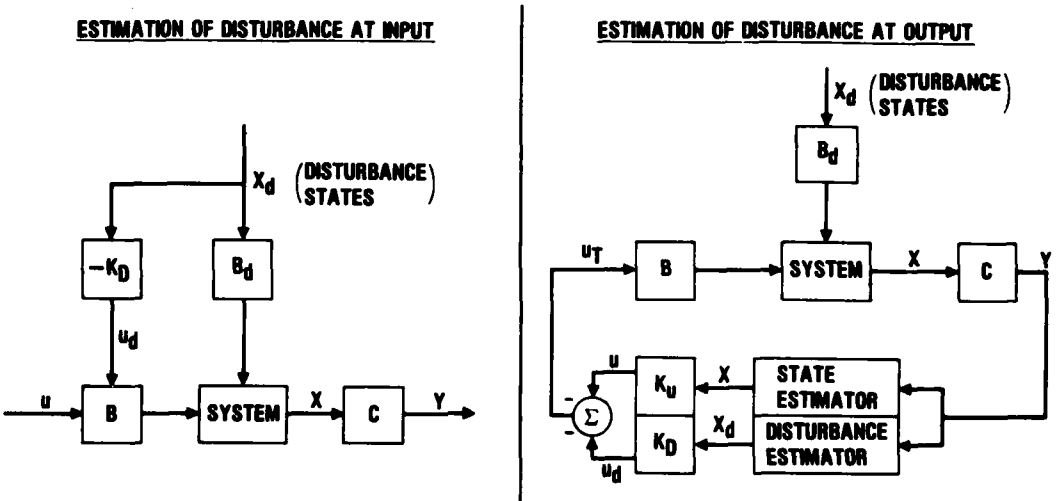

264 760-1

Figure 2-37. Disturbance Accommodation Techniques

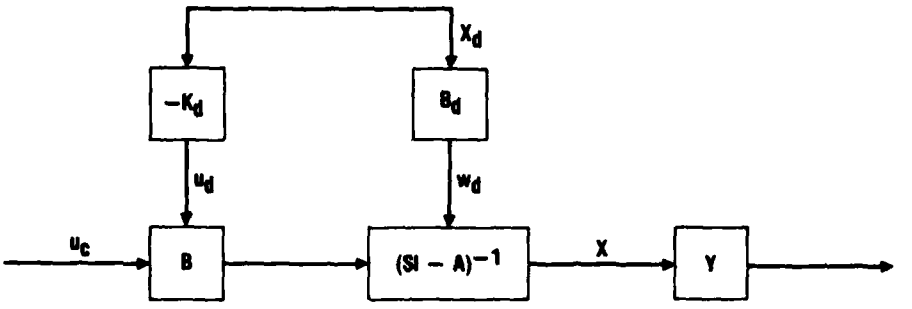

ACCOMMODATION EQUATION: u_d **MUST CANCEL** w_d **FOR ANY** X_d

$$B_d X_d - BK_d X_d = 0 \qquad (1)$$

OR

$$B_d - BK_d = 0 \qquad (2)$$

264 760-2

Figure 2-38. Input Disturbance Accommodation

Equation (3) is the disturbance accommodating equation.

As noted, input disturbance accommodation is an open-loop technique. The accommodation equation is static in nature. Another strength of the procedure is that it allows the closed-loop damping control, u_c, to be implemented independently of the disturbance control.

The disturbance accommodation loop is easily analyzed by transfer functions. The accommodation loop modifies the input matrix B_d. Thus, exact satisfaction of the accommodation equation (3) will result in zero disturbance effects at the system output, as shown in Figure 2-39.

The exact solution of the accommodation equation requires inversion of the input matrix B. In general, this matrix does not have an inverse; however, when the number of actuators equals the number of controlled modes, an exact solution for the accommodation equation may be obtained by following the procedure outlined in Table 2-3.

NO DISTURBANCE ACCOMMODATION

$$Y = C(SI - A)^{-1}B_d X_d \qquad (1)$$

DISTURBANCE ACCOMMODATION

$$Y = C(SI - A)^{-1}(B_d - BK_d)X_d \qquad (2)$$

THUS

$$B_d - (B_d - BK_d) = 0 \qquad (3)$$

FOR PARAMETER VARIATIONS:

$$B_d \rightarrow B_d + \Delta B_d \qquad (4)$$

$$B \rightarrow B + \Delta B \qquad (5)$$

THUS

$$(B_d - BK_d) - [B_d + \Delta B_d - (B + B\Delta)K_d] = [\Delta B_d - \Delta BK_d] \neq 0$$

264 760-3

Figure 2-39. Disturbance Accommodated Transfer Function

To clarify the procedure just outlined, a sample problem is presented, Table 2-4. The example illustrates the form of B^{-1} and how exact satisfaction of the accommodation equation is obtained.

Table 2-3. Disturbance Accommodation Solution Procedure

$$B_d - BK_d = 0 \qquad (1)$$

OR

$$K_D = B^{-1}B_d \qquad (2)$$

IN GENERAL, B IS NOT INVERTIBLE. HOWEVER, WE WANT AN EXACT SOLUTION FOR K_D (NO GENERALIZED INVERSE). THUS, WE DO THE FOLLOWING OPERATIONS:

1) **FORM $\bar{B}$ BY DELETING ZERO ROWS FROM B AND B_d**

2) **CAUSE $\bar{B}$ TO BE SQUARE BY MAKING THE NUMBER OF ACTUATORS TO EQUAL THE NUMBER OF MODES TO BE CONTROLLED**

3) **INVERT $\bar{B}$ (WE PLACE ACTUATORS TO ASSURE THE INVERTIBILITY OF $\bar{B}$)**

4) **INSERT CORRESPONDING ZERO COLUMNS INTO $\bar{B}^{-1}$ FORMING B^{-1}**

As with any open-loop technique disturbance accommodation may be sensitive to parameter variations. The disturbance accommodation equation can be desensitized against parameter variations by adding additional actuators such that the original input matrix (which had our special inverse) is imbedded in a larger matrix. This desensitization phenomenon can be explained by two effects: reduced gain level and signal averaging. If we add additional actuators, the same general actuation level may be attained with lower gains. Also, as sensor and actuator signals are now received from, and applied to, a larger area of the structure parameter variations tend to "average out."

The desensitization effect can be further enhanced if one has a-priori information of areas of the structure that are uncertain: one simply selects the weighting matrix R to cause small gains for the troublesome areas. (This weighting-matrix procedure was <u>not</u> used for the Draper evaluation structure because it violated the ground rules.)

To derive the desensitized disturbance gains we assume the number of actuators exceeds the number of controlled modes, but in placing our actuators we retain a square invertible matrix, B_1 (n x n) which has rank equal to the number of controlled modes. Thus B_1 is imbedded in the larger actuator matrix, B (2n x r), and we now proceed to solve this augmented filter accommodation equation for the disturbance gain matrix K_d. The procedure is detailed in Table 2-5; where we employ a specific optimal control format thereby generalizing a procedure given by Kwaakernak and Silvan, p. 262, Reference 17; i.e., P_{12} is a submatrix of the Riccati equation. We also note that the solution obtained for K_d is exact.

2.9 INPUT-OUTPUT DECENTRALIZATION

We now take advantage of the many actuators required for disturbance accommodation to design a completely decoupled control law such that each mode is controlled by a separate gain element (Reference 22). As both B and C are invertable in the sense indicated, and we have an actuator/sensor pair for each mode, no estimator is required. This leads to a simple closed-loop controller of increased robustness.

Figure 2-4 illustrates the concept where we show the inversion of the input and output matrix in conjunction with a diagonal feedback gain matrix; i.e., the actual system gains are given by the matrix $(-B^{-1} K C^{-1})$.

The effects of input-out decentralization are easily analyzed in state variable form. The matrix inversions for B and C effectively eliminate these matrices from the dynamic equations. If the gain matrix, K, is diagonal then each mode is separately controlled, i.e., we have completely decoupled control. Figure 2-41 illustrates the procedure.

Table 2-4. Sample Calculation of the Disturbance Accommodating Gain, K_d

GIVEN B, B_d: FIND K_D

$$B_d = \begin{bmatrix} 0 & 0 \\ 0 & 2 \\ 0 & 0 \\ 0 & 4 \end{bmatrix} \quad ; \quad B = \begin{bmatrix} 0 & 0 \\ 1 & 1 \\ 0 & 0 \\ 3 & 4 \end{bmatrix} \qquad (1)$$

REMOVING ZERO ROWS YIELDS

$$\bar{B}_d = \begin{bmatrix} 0 & 2 \\ 0 & 4 \end{bmatrix} \quad ; \quad \bar{B} = \begin{bmatrix} 1 & 1 \\ 3 & 4 \end{bmatrix} \qquad (2)$$

INVERTING B YIELDS

$$B^{-1} = \begin{bmatrix} 4 & -1 \\ -3 & 1 \end{bmatrix} \qquad (4)$$

PLACE ZERO COLUMNS IN B^{-1}, THUS

$$B^{-1} = \begin{bmatrix} 0 & 4 & 0 & -1 \\ 0 & -3 & 0 & 1 \end{bmatrix} \qquad (5)$$

NOW CALCULATE $K_D = B^{-1}B_d$

$$K_d = \begin{bmatrix} 0 & 4 & 0 & -1 \\ 0 & -3 & 0 & 1 \end{bmatrix} \begin{bmatrix} 0 & 0 \\ 0 & 2 \\ 0 & 0 \\ 0 & 4 \end{bmatrix} = \begin{bmatrix} 0 & 4 \\ 0 & -2 \end{bmatrix} \qquad (6)$$

CHECK ($B^{-1}B = I$)

$$B^{-1}B = \begin{bmatrix} 0 & 3 & 0 & -1 \\ 0 & -3 & 0 & 1 \end{bmatrix} \begin{bmatrix} 0 & 0 \\ 1 & 1 \\ 0 & 0 \\ 3 & 4 \end{bmatrix} = \begin{bmatrix} 1 & 0 \\ 0 & 1 \end{bmatrix} \qquad (7)$$

CHECK ($B_d = BK_d$)

$$B_d = \begin{bmatrix} 0 & 0 \\ 0 & 2 \\ 0 & 0 \\ 0 & 4 \end{bmatrix} = \begin{bmatrix} 0 & 0 \\ 1 & 1 \\ 0 & 0 \\ 3 & 4 \end{bmatrix} \begin{bmatrix} 0 & 4 \\ 0 & -2 \end{bmatrix} = \begin{bmatrix} 0 & 0 \\ 0 & 2 \\ 0 & 0 \\ 0 & 4 \end{bmatrix} \qquad (8)$$

264.760-5

Table 2-5. Desensitizing Effect of Additional Actuators

LET THE NUMBER OF ACTUATORS EXCEED THE NUMBER OF MODES, BUT WE RETAIN OUR SQUARE INVERTIBLE MATRIX

$$B_1(N \times N) - B(2N \times R) = [B_1\ B_2];\ B^{-1}\ \text{EXISTS},\ R > N \qquad (1)$$

NOW SOLVE THE ACCOMMODATION EQUATION BY GENERALIZED INVERSE AND SPECIFIC OPTIMAL CONTROL FORMAT

OR	$K_d = R^{-1}B^T P_{12}$	(2)
AND	$BK_D = BR^{-1}B^T P_{12} = B_d$	(3)
THUS	$P_{12} = [BR^{-1}B^T]^{-1}B_d$	(4)
LET (R = I)	$K_D = R^{-1}B^T[BR^{-1}B^T]^{-1}B_d$	(5)
AND	$K_D = B^T[BB^T]^{-1}B_d$	(6)
	$B_d = BK_d$ (EXACT SOLUTION)	(7)

264.760-6

2.10 BANDWIDTH REDUCTION AND DISTURBANCE ACCOMMODATION

The disturbance control, u_d, and the closed-loop control, u_c, are independent of each other. Thus, u_c can be designed by any means available to the designer, optimal, suboptimal or classical means. Of special interest is the design of low bandwidth systems via input/output decentralization. Such decoupled systems will provide greater robustness in the face of severe parameter variations.

Transfer function analysis also reflects this independence of u_c and u_d. The disturbance control modifies the input matrix, B_d. The closed-loop control modifies the plant matrix, A. Both modifications appear as independent multiplicative factors in the transfer function, as shown in Figure 2-42.

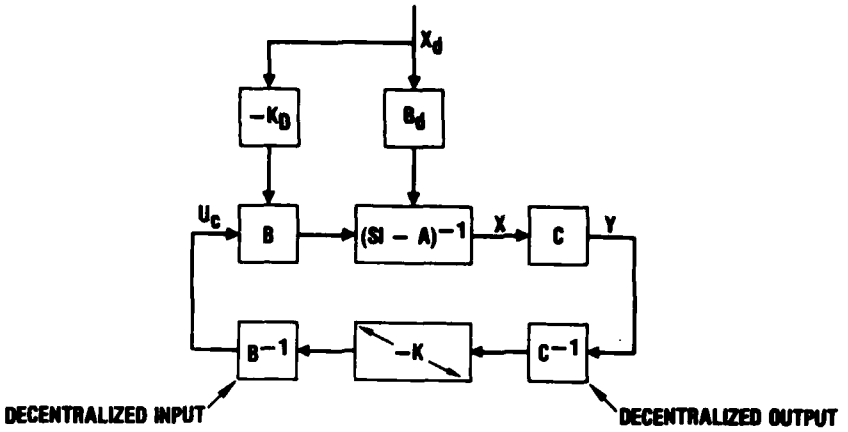

264 760-7

Figure 2-40. Input-Output Decentralization for Decoupled Control

$$\dot{X} = Ax + Bu \quad (1)$$

$$Y = Cx \quad (2)$$

$$U_c = -B^{-1}KC^{-1}Y = -B^{-1}KC^{-1}CX = -B^{-1}KX \quad (3)$$

THUS

$$\dot{X} = Ax + B(-B^{-1}KX) \quad (4)$$

$$\dot{X} = Ax - KX \quad (5)$$

ASSUMING A DIAGONAL GAIN MATRIX YIELDS DECOUPLED CONTROL
(EACH GAIN AFFECTS ONLY ONE MODE)

$$\begin{bmatrix} \dot{X}_1 \\ \dot{X}_2 \\ \dot{X}_3 \\ \dot{X}_4 \end{bmatrix} = \begin{bmatrix} 0 & 1 & 0 & 0 \\ -\omega_1^2 & -2\zeta_1\omega_1 & 0 & 0 \\ 0 & 0 & 0 & 1 \\ 0 & 0 & -\omega_2^2 & -2\zeta_2\omega_2 \end{bmatrix} \begin{bmatrix} X_1 \\ X_2 \\ X_3 \\ X_4 \end{bmatrix} - \begin{bmatrix} 0 & 0 & 0 & 0 \\ 0 & Kv_1 & 0 & 0 \\ 0 & 0 & 0 & 0 \\ 0 & 0 & 0 & Kv_2 \end{bmatrix} \begin{bmatrix} X_1 \\ X_2 \\ X_3 \\ X_4 \end{bmatrix} \quad (6)$$

264 760-8

Figure 2-41. Effect of Input-Output Decentralization

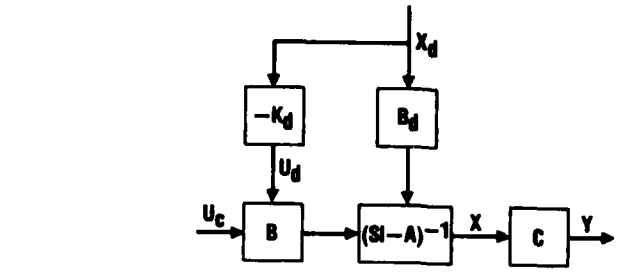

CLOSED-LOOP TRANSFER FUNCTION

$$Y = C(SI - A_{CL})^{-1}(B_d - BK_d)X_d$$

FREQUENCY RESPONSE

DISTURBANCE CONTROL

264 760-9

Figure 2-42. Simultaneous Bandwidth Reduction and Disturbance Accommodation

SECTION 3

ANALYSIS AND SIMULATION

The purpose of the analysis and simulation task was to evaluate the applicability of the theory to complex structure. Since erroneous conclusions can be drawn from evaluations using too-simple models, the complexity of the structural model is an essential feature of this task.

3.1 DRAPER MODEL #2

In order to provide a realistic testbed for control system evaluation, the Charles Stark Draper Laboratory developed the system model shown in Figure 3-1 and described in detail in Reference 3. This model consists of a flexible optical support structure and an isolated equipment section which contains solar panels. Optical support structure consists of the upper mirror support truss, lower mirror support truss, and the metering truss which maintains mirror separation. The finite element model is shown in Figure 3-2. The structure is configured as a truss, but it is assumed that all joints allow a full moment connection. Thus, both bending and axial stiffness are included in the model for all structural members. To evaluate system performance two classes of disturbances (parameter variations and oscillatory equipment vibrations) are included for application to the model.

3.1.1 PARAMETER VARIATIONS. To assess the sensitivity of the control system to modeling errors and manufacturing tolerances two sets of physical parameter variations are employed. These variations are summarized in Table 3-1. The changes are confined to the optical support structure and involve mass distribution changes on the upper optical support truss and stiffness changes in the metering truss. These parameters are chosen based on their impact on LOS error in several critical modes. The amount of variation is driven by the desire to vary the natural frequencies by 10%.

Dynamic analyses were conducted on both perturbed models using NASTRAN. The resulting natural frequencies are given in Table 3-2 along with those of the original model. The results show that both sets of parameter variations had more impact on the higher frequency modes because the upper support truss and the metering truss contain a higher percentage of the total energy in these modes than in the lower modes.

3.1.2 SYSTEM DISTURBANCES AND OPTICAL TOLERANCES. The disturbance model consists of two sinusoidal forces which are applied to a point on the optical support structure and a point on the equipment section. These forces simulate onboard vibrating equipment. It is assumed that both forces will act simultaneously.

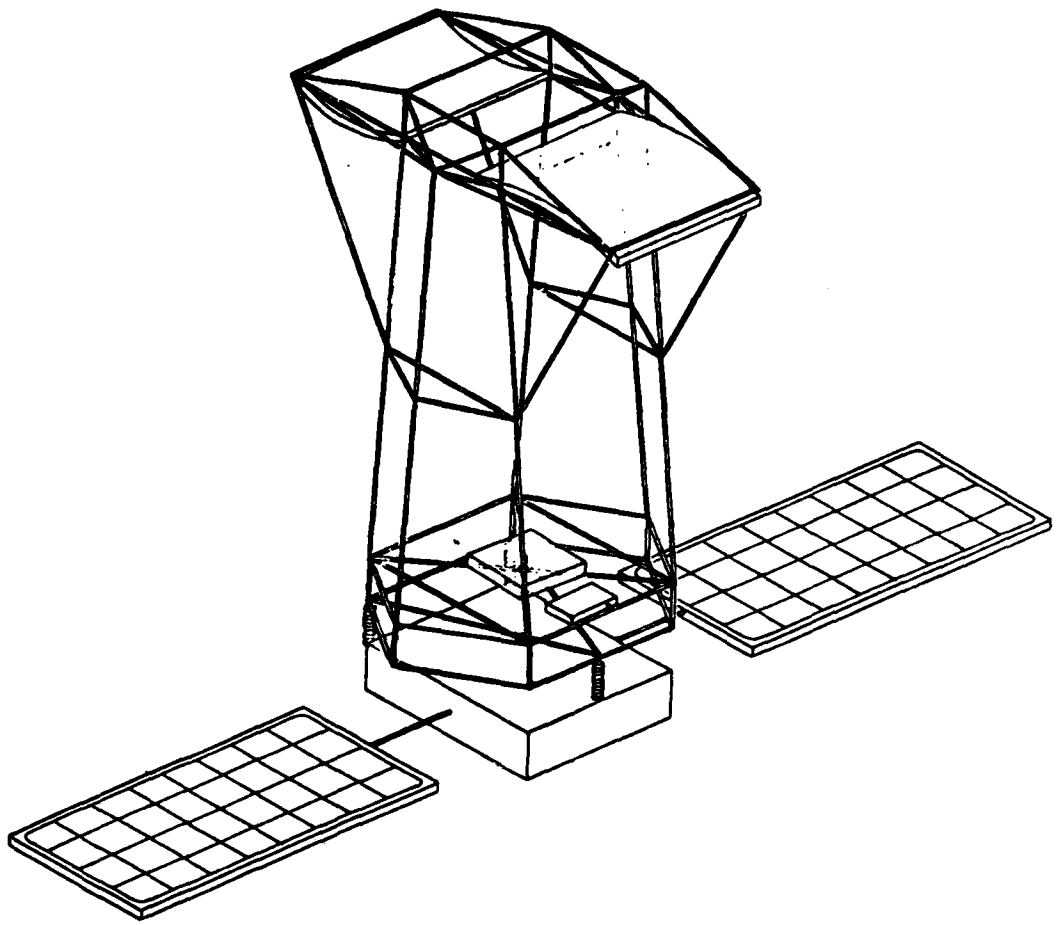

264.760-15

Figure 3-1. Nominal Draper Evaluation Model

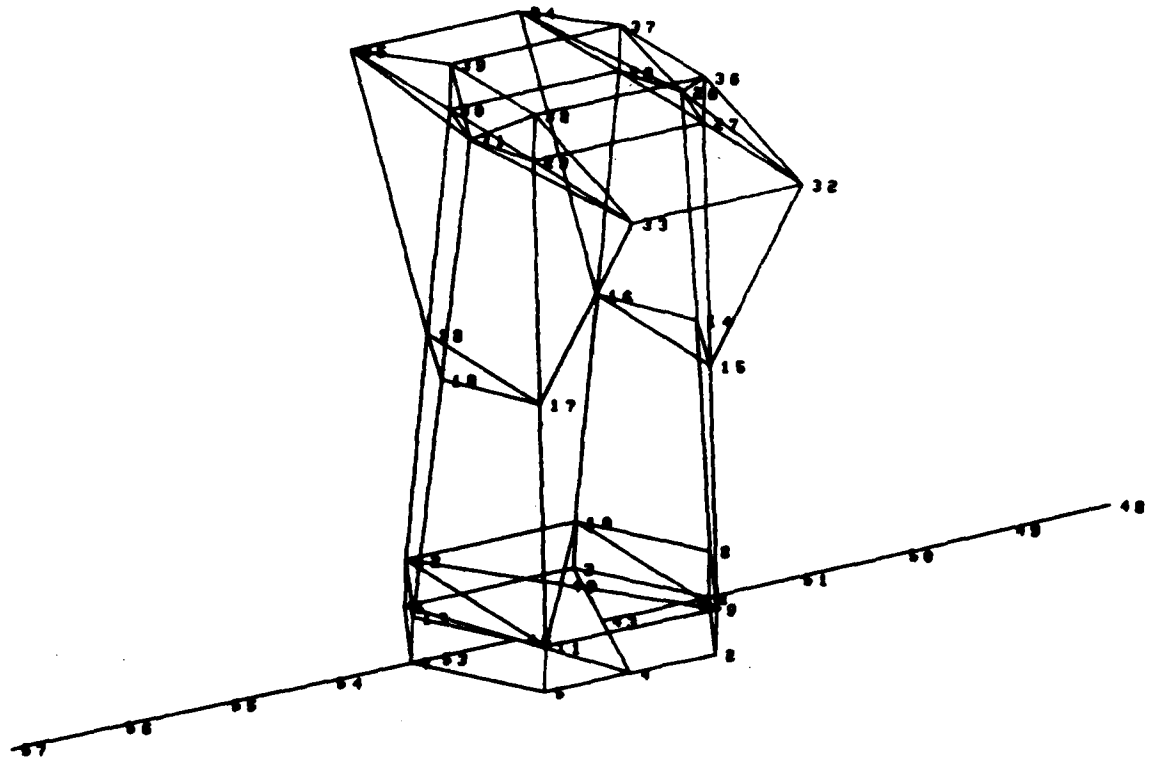

264.760-16

Figure 3-2. Finite-Element Model of the Nominal Draper System

Table 3-1. Parameter Variations for the Nominal Draper Evaluation Model

- **MASS CHANGES**

NODE	ORIGINAL MASS	CASE #2 — 2A	CASE #4 — 4A
27	375.0	350.0	375.0
28	375.0	350.0	350.0
29	375.0	350.0	350.0
30	375.0	350.0	350.0
32	500.0	500.0	550.0
33	500.0	550.0	450.0
34	250.0	300.0	300.0
35	250.0	250.0	200.0

- **STIFFNESS CHANGES**

MEMB	NA	NB	SECTION PROPERTY # CASE 2A	CASE 4A
76	8	15	1	1
80	9	15	1	1
81	11	17	1	1
85	13	19	1	2
99	15	32	1	2
101	17	33	1	2

- **SECTION PROPERTIES**

#1 — 25cm DIA. × 0.10 cm ROUND TUBE

$A = 7.823 \times 10^{-4}\ m^2$

$I = 6.063 \times 10^{-6}\ m^4$

$J = 1.213 \times 10^{-5}\ m^4$

#2 — 25cm DIA. × 0.025 cm ROUND TUBE

$A = 1.962 \times 10^{-4}\ m^2$

$I = 1.529 \times 10^{-6}\ m^4$

$J = 3.059 \times 10^{-6}\ m^4$

264.760-10

Table 3-2. Modal Survey for the Draper Evaluation Model (Parameter Variations Included)

MODE	ORIGINAL	CASE #2	CASE #4
1-6	0.0	0.0	0.0
7	0.1455	0.1455	0.1455
8	0.2632	0.2616	0.2632
9	0.3173	0.3172	0.3173
10	0.3329	0.3328	0.3329
11	0.4432	0.4432	0.4432
12	0.5779	0.5764	0.5778
13	0.5814	0.5815	0.5815
14	1.224	1.224	1.224
15	1.300	1.301	1.299
16	1.348	1.348	1.348
17	1.721	1.764	1.699
18	1.819	1.819	1.819
19	1.819	1.819	1.819
20	1.889	1.889	1.889
21	2.363	2.430	2.339
22	2.990	2.990	2.989
23	3.176	3.176	3.176
24	3.387	3.387	3.387
25	5.162	5.162	5.162
26	5.260	5.260	5.260
27	7.877	7.877	6.798
28	8.117	8.360	7.877
29	8.360	8.567	8.360
30	8.571	8.813	8.813
31	8.813	8.813	8.813
32	8.813	9.522	9.246
33	11.346	11.346	11.346
34	11.498	11.575	11.469
35	12.726	12.882	12.492
36	13.583	13.583	13.046
37	13.714	13.875	13.583
38	14.160	14.278	13.634
39	15.652	16.323	14.212
40	16.072	16.945	15.262
41	16.525	17.077	15.693
42	16.745	17.266	15.884
43	17.155	19.321	16.724
44	17.828	20.064	17.897
45	19.071	20.994	20.035
46	23.772	25.071	23.819
47	24.419	25.204	24.671
48	25.909	25.952	25.482
49	26.363	26.429	26.201
50	26.429	27.322	26.429

The larger of the two is located at node 46 on the equipment section. A smaller amplitude disturbance is located at node 37 on the optical support truss. Both forces act in the z-direction and are assumed to act independently. The amplitude, frequency, and direction of each are given by Figure 3-3.

Damping is assumed to be 0.1% in all modes except the isolator modes (7, 8, 11, 12, 13, 16) which are assumed to have 50.% damping due to the isolator. The tolerances for system line of sight error and defocus are

$$\text{LOS} = 1.0 \times 10^{-6} \text{ radians}$$

$$\text{Defocus} = 5.0 \times 10^{-4} \text{ meters}$$

3.1.3 PROBLEM DESCRIPTION. The control problem as presented by Draper Model Number 2 may now be stated as: Design a control system for the nominal structure which counteracts the two sinusoidal disturbances and meets the LOS requirements. Evaluate system performance in the face of the enumerated parameter variations.

3.2 INITIAL PROBLEM EVALUATION

Rather than proceeding directly to active system design, an initial evaluation of the problem was made as follows:

1) Conduct an LOS analysis and rank modes according to LOS contribution.

2) Arbitrarily add 20% damping to all modes for test runs to evaluate potential role of damping.

3) Use actuator placement algorithm to provide input matrices of the proper rank.

4) Initially accommodate all modes and then delete mode by mode according to LOS ranking.

5) Add actuators to provide desensitization.

6) Analyze perturbed systems to determine the additional amount of attenuation required to meet specifications.

7) Design reduced bandwidth system.

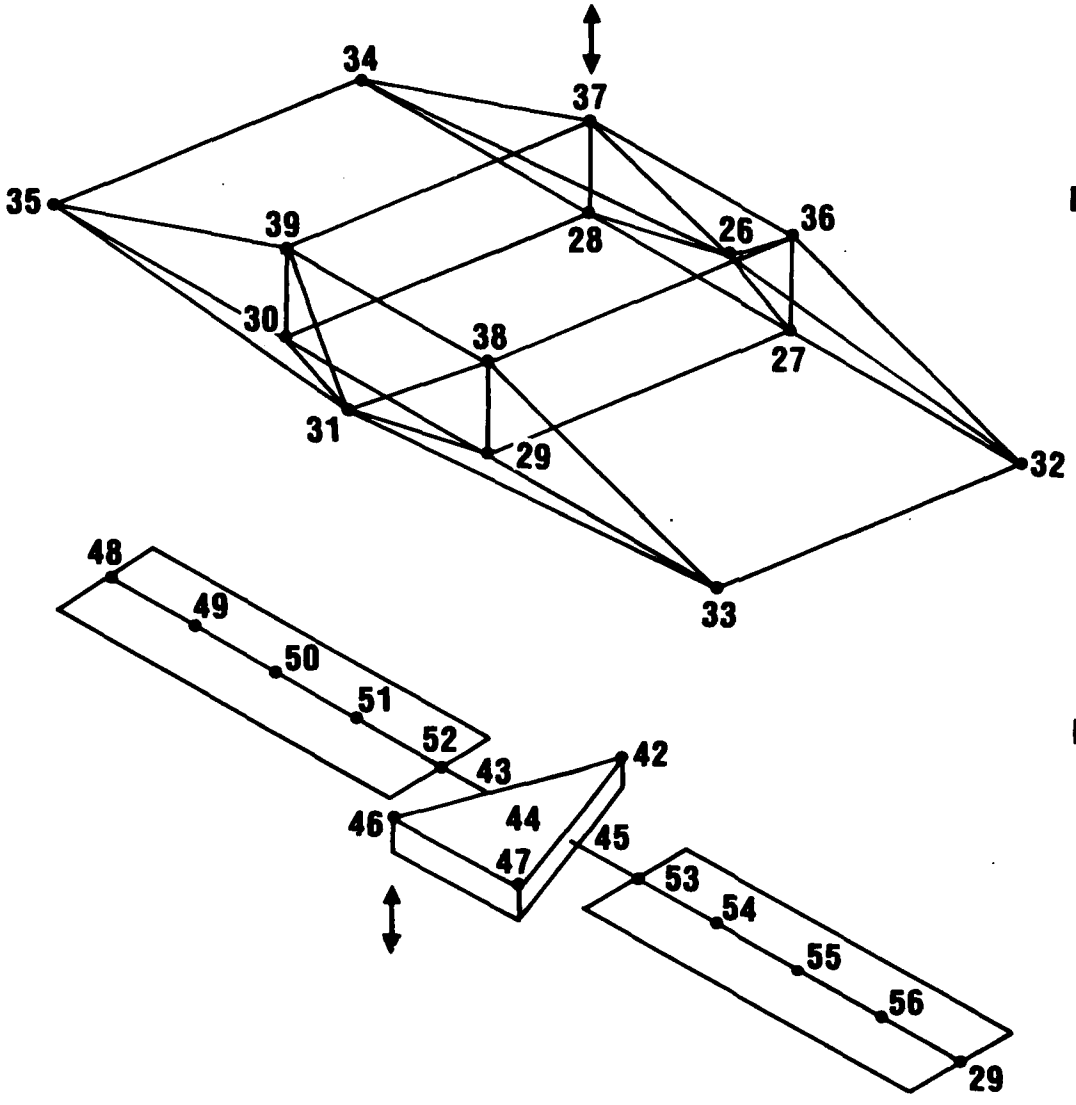

F_{37} = A SINωt

A = 200 NEWTONS

ω = 62.83 RAD/SEC (10.0 Hz)

F_{46} = A SINωt

A = 400 NEWTONS

ω = 31.42 RAD/SEC (5.00 Hz)

264.760-12

Figure 3-3 Disturbances Applied to the Draper Structure

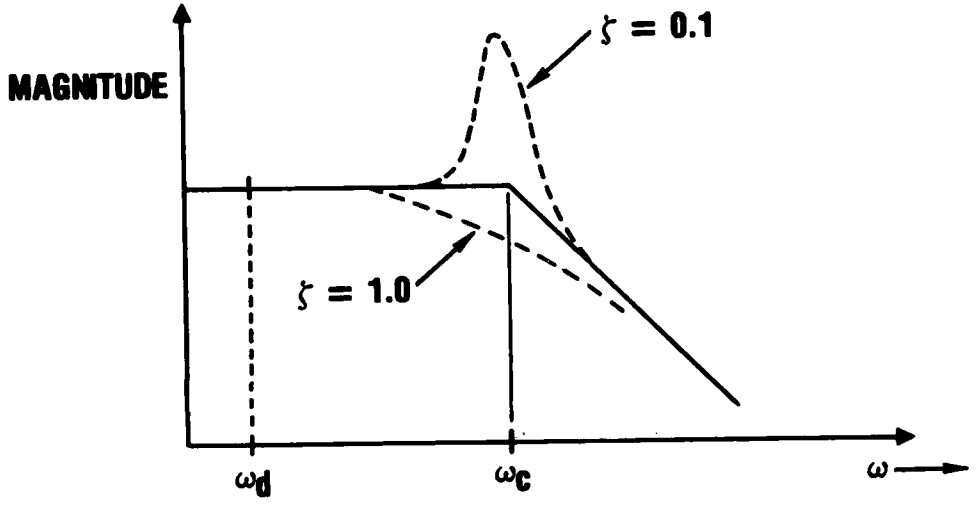

264.760-13

Figure 3-4. Modal Response and Disturbance Frequency

This evaluation resulted in the following conclusions:

1) Modal damping will not provide disturbance control for this system.

2) Disturbance accommodation requires feedforward control of 43 modes. (Mode 50 is residual.)

3) Disturbance accommodation and system bandwidth reduction will be required to meet specs with parameter variation, but bandwidth reduction is so large that a high gain system results with the usual sensitivity problems.

The negligible effect of damping on the performance characteristics may be explained as follows: The disturbance frequencies at 5 and 10 hertz lie well below the resonant frequencies of many modes. Thus for this situation the modal transfer functions respond as essentially constant gains and the disturbances are transmitted to the line of sight scaled by the low frequency modal gain, i.e., the modes act as rigid links to the LOS. This situation is illustrated in Figure 3-4. One obvious way to correct this situation is the lowering of the low frequency modal gain by closed-loop means. This may be accomplished by acceleration feedback integrated into our decoupled control scheme.

3.3 DISTURBANCE ACCOMMODATED DESIGNS

Four different designs for the Draper evaluation structure are presented. Design I involves standard disturbance accommodation and employs 43 actuators. Design II involves standard disturbance accommodation and employs 153 actuators. The additional actuators are added to provide desensitization for the disturbance accommodation algorithm. Damping is injected in open-loop fashion so as to check the efficiency of disturbance accommodation without adding the additional variable of closed-loop behavior. Design III incorporates closed-loop bandwidth reduction in addition to basic disturbance accommodation. Finally, Design I-A (an iteration on the first design) provides 20% damping via closed-loop decoupled control. The final design remains stable, but is out of spec for the perturbed models. Table 3-3 summarizes the different designs and results.

Numerical evaluation data for each of the designs is shown in Table 3-4. Examination of the table reveals that each of the designs easily meets specifications by several orders of magnitude: i.e., nominal LOS values for Designs I, IA, and III are on the order of 10^{-14} radians. The LOS values for Design III, the low frequency design, are on the order of 10^{-18} radians. However, all designs are out of specification for the parameter variations. The best performance, with respect to

Table 3-3. Disturbance Accommodation Designs

DESIGN I • 43 ACTUATOR/SENSOR PAIRS — 43 CONTROLLED MODES — 1 RESIDUAL MODE (MODE 50) — 20% VELOCITY DAMPING — OPEN LOOP	**SUMMARY** NOMINAL MODEL: EXCEEDS SPECIFICATIONS PERTURBED MODEL II: OUT OF SPECIFICATION PERTURBED MODEL IV: OUT OF SPECIFICATION ALL MODELS STABLE
DESIGN II • 153 ACTUATOR/SENSOR PAIRS — 43 CONTROLLED MODES — 1 RESIDUAL MODE (MODE 50) — 20% VELOCITY DAMPING — OPEN LOOP	**SUMMARY** NOMINAL MODEL, EXCEEDS SPECIFICATIONS PERTURBED MODEL II: OUT OF SPECIFICATION PERTURBED MODEL IV: OUT OF SPECIFICATION ALL MODELS STABLE PERFORMANCE SUPERIOR TO THAT OF 43 ACTUATOR DESIGNS
DESIGN III • 43 ACTUATOR/SENSOR PAIRS • BANDWIDTH REDUCTION BY ACCELERATION FEEDBACK — 43 CONTROLLED MODES — 1 RESIDUAL MODE (MODE 50) — VELOCITY FEEDBACK (20% DAMPING) — CLOSED LOOP — BANDWIDTH = 3.1×10^{-2} RADIANS	**SUMMARY** NOMINAL DESIGN EXCEEDS SPECIFICATIONS PERTURBED DESIGNS DO NOT TOLERATE PARAMETER VARIATIONS BANDWIDTH REDUCTION GAINS ARE EXCESSIVE
DESIGN I-A • CLOSED-LOOP DECOUPLED CONTROL FOR DESIGN I • VELOCITY FEEDBACK 20% DAMPING • 43 ACTUATOR/SENSOR PAIRS — 43 CONTROLLED MODES — 1 RESIDUAL MODE (MODE 50)	**SUMMARY** NOMINAL MODEL: EXCEEDS SPECIFICATIONS PERTURBED MODEL II: OUT OF SPECIFICATION PERTURBED MODEL IV: OUT OF SPECIFICATION ALL MODELS STABLE

264.760-14

Table 3-4. Numerical Evaluation of Design Data

	DESIGN I						DESIGN IA					
	NOMINAL		PERT #2		PERT #4		NOMINAL		PERT #2		PERT #4	
	5 Hz	10 Hz	5 Hz	10 Hz	5 Hz	10 Hz	5 Hz	10 Hz	5 Hz	10 Hz	5 Hz	10 Hz
LOS X	7.0E-14	7.0E-13	4.5E-2	2.0E-1	7.8E-3	9.0E-2	7.0E-15	1.4E-14	6.2E-6	2.0E-4	1.4E-4	2.0E-4
LOS Y	1.0E-13	7.5E-14	1.4E-1	4.0E-2	3.7E-2	2.0E-2	4.0E-13	4.8E-14	1.2E-4	1.8E-5	2.7E-5	1.8E-4
DEFOCUS	9.6E-14	1.7E-13	5.0E-2	2.5E-2	2.5E-2	3.7E-2	6.0E-15	9.0E-15	1.5E-4	1.3E-4	1.5E-4	4.5E-5

	DESIGN II						DESIGN III	
	NOMINAL		PERT #2		PERT #4		NOMINAL	
	5 Hz	10 Hz	5 Hz	10 Hz	5 Hz	10 Hz	5 Hz	10 Hz
LOS X	1.7E-14	6.0E-14	1.4E-6	2.5E-6	8.0E-6	4.6E-6	2.9E-17	1.0E-20
LOS Y	7.0E-15	8.0E-15	3.6E-6	8.0E-7	3.0E-5	2.9E-6	4.8E-16	6.5E-20
DEFOCUS	2.5E-14	1.6E-14	1.1E-6	1.9E-6	1.5E-5	3.9E-6	6.5E-18	2.8E-21

SPECIFICATION
LOS = 1.0E-6 RADIAN
DEFOCUS = 5.0E-4 METER

DESIGN I: 43 ACTUATORS (20% OPEN-LOOP DAMPING)
DESIGN IA: 43 ACTUATORS (20% CLOSED-LOOP DAMPING)
DESIGN II: 153 ACTUATORS (20% OPEN-LOOP DAMPING)
DESIGN III: 43 ACTUATORS (CLOSED-LOOP LOW FREQUENCY)

264.760-18

parameter variation, is provided by Design II. The LOS error is on the order of 10^{-6} radian.

3.4 SYSTEM DESIGN COMMENTS

As a result of the analysis and simulation activities using the Draper optical system model, it became apparent that the system design approach of designing the structure first and then adding the controls as an "after thought" has severe limitations for precision space systems. The best approach would be one where the structure and the control system are designed concurrently so to give an optimum combination of structure and control. However, since the technology for the best approach is not presently available, it would appear appropriate to at least re-examine the structure for possible improvements where it is found that modal damping will not provide a sufficiently quiet optical environment to meet requirements.

The Draper evaluation structure exemplifies this viewpoint. The disturbances at nodes 37 and 46 are strongly coupled to the line of sight. Several simple and economical structural design changes can attenuate the disturbance transmission characteristics such that an active control system can then be appropriately employed to meet mission requirements. This conclusion was reached after observing the effect of the disturbance accommodation algorithm: i.e., it appears to be attempting to redesign the structure, via input matrix manipulation, as viewed from the disturbance ports. When this situation arises, it appears intuitively more efficient to attack the problem at its primary source, the structural design process, rather than indirectly through the control system in ad hoc fashion.

The key phrase in the above discussion is "modal damping". Again, it becomes evident during the controller design process that control techniques designed primarily for modal damping do not provide an adequate design basis for those classes of systems that do not respond to damping techniques. Thus, the Draper model calls attention to the fact that multivariable control algorithms, which incorporate disturbance accommodation to complement modal damping, may be required for certain classes of LSS control problems. This poses an interesting area for future research especially in the arena of LQG design.

SECTION 4

DEMONSTRATION PLANNING

Analyses and computer simulations, while extremely valuable in investigating the applicability of control theory, do not provide the same confidence as a comprehensive demonstration and evaluation test using real hardware. However, the question of the comprehensiveness of the demonstration must be considered. The particular structural configuration used in the test could represent an easy problem for the theory and false confidence in the ability of the theory to handle other configurations might result.

The purpose of the Demonstration Planning task was to identify the various structural elements which should be included in a comprehensive test article and then design such a test article. Control actuator installation and structural test article suspension are also included in the task. The following were established as goals:

a. Configuration shall be representative of typical, projected space structure systems.

b. Elements of the test structure shall be representative of projected space structure elements.

c. Test structure shall exhibit full spectrum of dynamic response and its dynamic characteristics shall be sufficiently severe and complex that the full capability of the control system shall be adequately demonstrated.

d. Test structure shall have provisions for installation of devices for propagating, sensing and controlling dynamic disturbance.

4.1 SURVEY OF SPACE STRUCTURE CONFIGURATIONS AND ELEMENTS

A survey of typical, projected space structure systems reveals that structural elements fall into four general categories:

a. "Plates" - for providing uniform, stable support to functional surfaces such as mirrors and R.F. reflectors. For large space systems these "plates" take the form of planar trusses.

b. Compression Members - for reacting axial and/or bending loads, i.e., struts and beams, (pin ended or built-in, and cantilevering).

c. Tension Members - for reacting axial tension loads only, i.e., cords and cables.

d. Biaxial Tension Members - provide flat, lightweight, stable surfaces; i.e., membranes.

Concepts surveyed are listed in Table 4-1 and briefly described below.

a. HALO/WALRUS (Struts and Ties)
A structural system with three major planar trusses stably located by a fully triangulated system of axially loaded struts and ties.

b. HALO/WALRUS (Cantilevering beams)
An alternative structural system consisting of cantilevering fixed-end beams acting as strut columns; stabilized in torsion by triangulated tension ties.

c. HALO/WALRUS (Monocoque shells)
Another structural approach using planar truss structures wrapped through 360° to form closed section "shells" which react loads in bending and in shear.

d. GEO-STATIONARY PLATFORM (Cantilevering beams)
Consists of six similar truss beams cantilevering from a common hub structure with payload systems at their tips.

e. "ADOPT" CASSEGRAIN OPTICAL CONCENTRATOR (Trusses and beams)
The primary optical surface is supported by a three-tier system of planar trusses and cantilever beams. The secondary optical surface is supported by converging beams cantilevered from the periphery of the main "primary" truss. A large, high frequency planar truss provides "foundation" structure for support of the primary optical surface. The interface between the planar truss and the primary optical surface involves second and third tiers of structure. The second tier is an array of truss "petals," and the third is a series of small planar trusses that directly support the optical panels. The "foundation" planar truss also provides support for the beams that support the system's secondary optical element.

f. FLEXIBLE FLYER (Trusses, beams, struts & ties)
This structural concept consists of a primary planar truss with two systems of triangulated struts and ties mounted on its periphery, one to support the secondary mirror and the other the equipment module. "Flying" struts are added to reduce the effective length of the major strut/beams. All struts are of the open truss type.

Table 4-1. Categories of Structural Element

CONCEPT	PLANAR TRUSS (PLATE)	COMPRESSION MEMBERS			TENSION MEMBER (TIE)	BI-AXIAL TENSION MEMBER (MEMBRANE)
		PIN-ENDED STRUT	FIXED-ENDED STRUT/BEAM	CANTILEVER STRUT BEAM		
A. HALO/WALRUS, TRIANGULAR	X	X			X	
B. HALO/WALRUS, CANTILEVER	X		X	X		
C. HALO/WALRUS, MONOCOQUE	X					
D. GEOSTATIONARY PLATFORM	X	X		X		
E. ADOPT	X	X	X	X		X
F. FLEXIBLE FLYER	X	X			X	X
G. M.R.S. RADIOMETER	X	X			X	X
H. MAYPOLE (HOOP & COLUMN)		X	X	X	X	X
I. LOFT (LOW FREQUENCY TELE)		X			X	
J. M.P.T.S	X					X

g. MILLIMETERWAVE RADIOMETER - M.R.S. (Struts, ties and membranes)
This 750-meter diameter system consists of a torus supporting a "geodesic dome" truss, which in turn, supports electrostatically shaped reflector membranes. Two pin-ended legs support the multiple feed assembly. Each leg consists of a multiplicity of pin-ended struts and cross braced tension ties. Four larger tension ties, installed as guy lines, complete the feed assembly support system.

h. "MAYPOLE" HOOP AND COLUMN (Struts, ties and membrane)
An efficient structural arrangement where diametric tension ties stabilize the compression hoop. For axial stability a central hub separates the ties fore and aft into conical orientation. The hub extends, telescopically, both in the fore and aft directions. The forward extension acts as a cantilever beam supporting the R.F. feed at its tip. A membrane, stretched within the hoop, is pulled into near paraboloidal shape by numerous tie lines anchored to the tip of the aft hub extension.

i. LARGE, LOW-FREQUENCY TELESCOPE-LOFT (Struts, ties and membrane)
A system of tie lines and membranes held in stable shape by centrifugal force. The axial components of the centrifugal forces are reacted by a single, compression element (mast) that is coincidental with the axis of rotation.

j. MICROWAVE POWER TRANSMISSION SYSTEM - MPTS (Truss, struts and membrane)
This structure is a NASA Johnson Space Center design for a Solar Power Satellite transmitting antenna. It is a planar truss a kilometer in diameter and consists of correspondingly large, component, pin-ended struts. Such struts may themselves be of open truss construction.

Conclusions to be drawn from the survey are that planar trusses are required in almost all concepts, followed by pin-ended struts, tension members (ties), biaxial tension members (membranes), cantilever beams and fixed ended strut/beams, in that descending order of utilization.

4.2 TEST ARTICLE DESCRIPTION

Having identified the required structural elements, the next step is to incorporate them into a structural test article. A strong candidate for representing the planar truss category is the Tetrahedral Truss concept. The tetrahedral truss geometry is recognized as a highly efficient space structure configuration, has been thoroughly characterized, and is likely to receive wide application. The structure of the MPTS concept is a very large example of this configuration.

Table 4-2 presents dynamic characteristics of a much smaller, eight bay tetrahedral truss. The thirty degree orientation of its intermediate (core) struts results in shallower structural depth and lower stiffness than the 45^{o} or 60^{o} orientations. Although the frequencies may change with size, depth, and material, the modal density should still be typical for a planar truss. Thus, the close grouping of certain modes (e.g., 7-8, 11-13, 19-20, 21-23, 31-32, 35-36, 38-39) shows that the tetrahedral truss has the potential for providing a satisfactorily complex control problem.

A tetrahedral truss design is included in candidate demonstration hardware designs presented below. As shown in Figure 4-1 it is an eight bay version, 3.0 meters (10 feet) in size, and is candidate for representing the planar truss (plate) category of space structure element. Material, sizes and proportions are selected to result in a first mode frequency below 50 Hz when 22.7 Kg (50 Lb) of parasitic mass are equally distributed over the face of the structure.

Due to its high degree of structural redundancy, individual strut elements of the truss may be removed without loss of structural integrity. Such removal, however, does reduce the stiffness of the structure. It is therefore feasible to adjust and modify the dynamic characteristics of the truss by discrete removal of appropriate members from any location in the structure. Taken to the extreme, this capability enables extensive modification to the structure, as shown in Figure 4-2.

Typical structural detail is shown in Figure 4-3. The component elements (tubes, sleeves and discs) are common throughout. The structure consists of thin-walled brass tubing, sleeves (serving as tube splices) and discs (serving as joint splices at the structural node points). Ease of fabrication and of subsequent modification is the driver in selection of brass. Silver soldering is selected for the structural joints. Soft silver solder should be used for the sleeved joints connecting the tubular elements to the "spiders," to facilitate possible subsequent removal. The use of soldered joints throughout minimizes the possibility of friction damping (slip) at the joints.

It is considered that any alternative joining technique based on mechanical clamping, bolting or pinning would be cumbersome, unreliable, and expensive and may result in erratic damping. There are 840 sleeved joints and the time and cost aspects of selecting, acquiring, installing and qualifying that number of mechanical clamping devices is likely to be unacceptable.

Tension ties and cantilever beams are represented as shown in Figure 4-4. The three dimensional truss beam is rigidly mounted on the planar truss at three interface node points. Two guy lines (tension ties) connect the tip of the cantilever to points on the periphery of the planar truss. By varying the pre-tension in the ties,

Table 4-2. Typical Planar Truss Modes

ERECTABLE ANTENNA NO BAYS= 8.000 40.000 DIA (FT)
AN (DEG) 30.00 F/D= 0.000 07/21/80

NORMAL MODES ANALYSIS FOR ACOSS7

MODE NO.	EXTRACTION ORDER	EIGENVALUE	REAL EIGENVALUES RADIANS	CYCLES
1	17	1.802941E+02	1.342737E+01	2.137032E+00
2	19	9.328638E+02	3.054282E+01	4.861041E+00
3	18	1.468334E+03	3.831884E+01	6.098634E+00
4	16	6.401685E+03	8.001053E+01	1.273407E+01
5	20	1.537789E+04	1.240076E+02	1.973642E+01
6	21	2.576730E+04	1.605220E+02	2.554787E+01
7	22	4.440934E+04	2.107352E+02	3.353955E+01
8	23	4.577132E+04	2.139423E+02	3.404998E+01
9	24	6.207398E+04	2.491465E+02	3.965290E+01
10	25	7.635825E+04	2.763300E+02	4.397928E+01
11	27	1.133447E+05	3.366670E+02	5.358223E+01
12	28	1.164474E+05	3.412439E+02	5.431066E+01
13	29	1.202941E+05	3.468344E+02	5.520041E+01
14	30	1.398239E+05	3.739303E+02	5.951287E+01
15	31	1.512760E+05	3.889421E+02	6.190206E+01
16	33	1.753371E+05	4.187327E+02	6.664338E+01
17	34	2.016603E+05	4.490660E+02	7.147108E+01
18	35	2.166632E+05	4.654710E+02	7.408201E+01
19	36	2.385313E+05	4.883967E+02	7.773075E+01
20	37	2.459523E+05	4.959357E+02	7.893063E+01
21	38	2.701142E+05	5.197251E+02	8.271683E+01
22	40	2.769749E+05	5.262840E+02	8.376071E+01
23	39	2.770912E+05	5.263945E+02	8.377830E+01
24	32	3.156092E+05	5.617911E+02	8.941183E+01
25	26	3.450302E+05	5.873927E+02	9.348645E+01
26	15	3.738592E+05	6.114402E+02	9.731374E+01
27	14	4.338695E+05	6.586877E+02	1.048334E+02
28	13	4.639241E+05	6.811197E+02	1.084036E+02
29	12	5.090622E+05	7.134860E+02	1.135548E+02
30	11	6.136833E+05	7.833794E+02	1.246787E+02
31	10	6.413474E+05	8.008417E+02	1.274579E+02
32	9	6.561792E+05	8.100489E+02	1.289233E+02
33	8	6.961500E+05	8.343560E+02	1.327919E+02
34	7	8.769003E+05	9.364295E+02	1.490374E+02
35	6	9.478964E+05	9.735997E+02	1.549532E+02
36	5	9.943752E+05	9.971836E+02	1.587067E+02
37	4	1.072888E+06	1.035803E+03	1.648532E+02
38	3	1.161280E+06	1.077627E+03	1.715097E+02
39	2	1.212700E+06	1.101226E+03	1.752656E+02
40	1	1.454852E+06	1.206173E+03	1.919683E+02

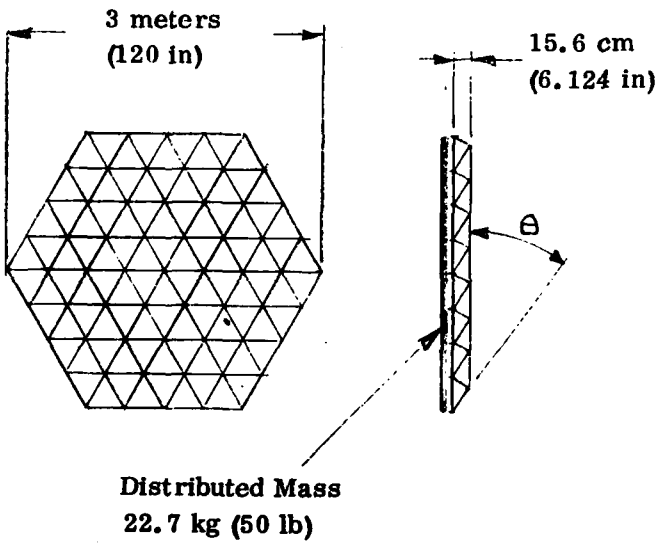

Length of face struts	0.38 m (15 in)
Length of core struts	0.27 m (10.6 in)
Dia. of struts	0.97 cm (.38 in)
Attitude of core struts (θ)	35.25°
No. of front face struts	(156)
No. of cone struts	(144)
No. of back face struts	(120)
Total length of tubing	144 m (472.2 ft)
Weight of structure	7.85 kg (17.3 lb)

Fundamental frequency 47.1 hz

Figure 4-1. Test Structure Configuration

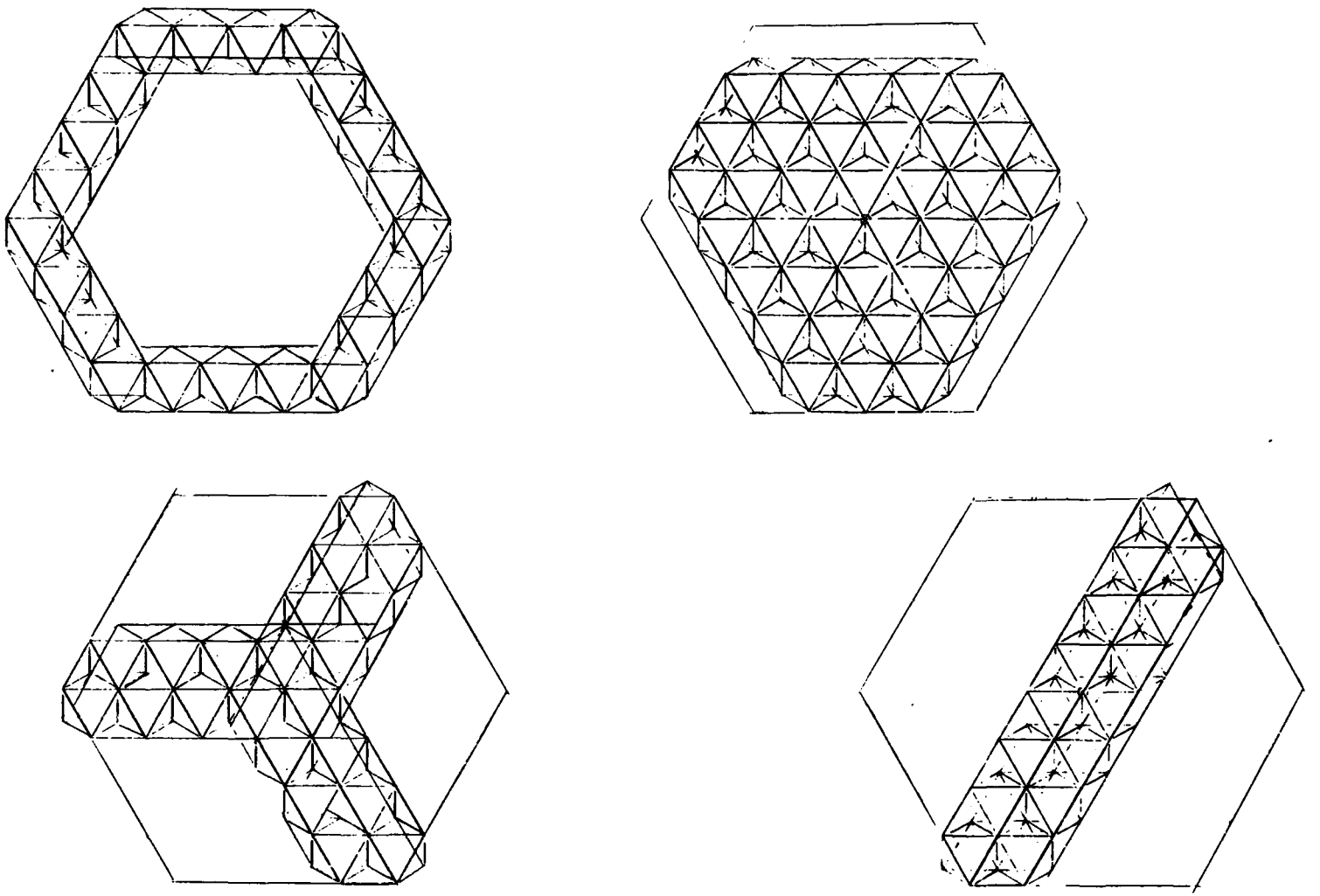

Figure 4-2. Planar Truss Configuration Options

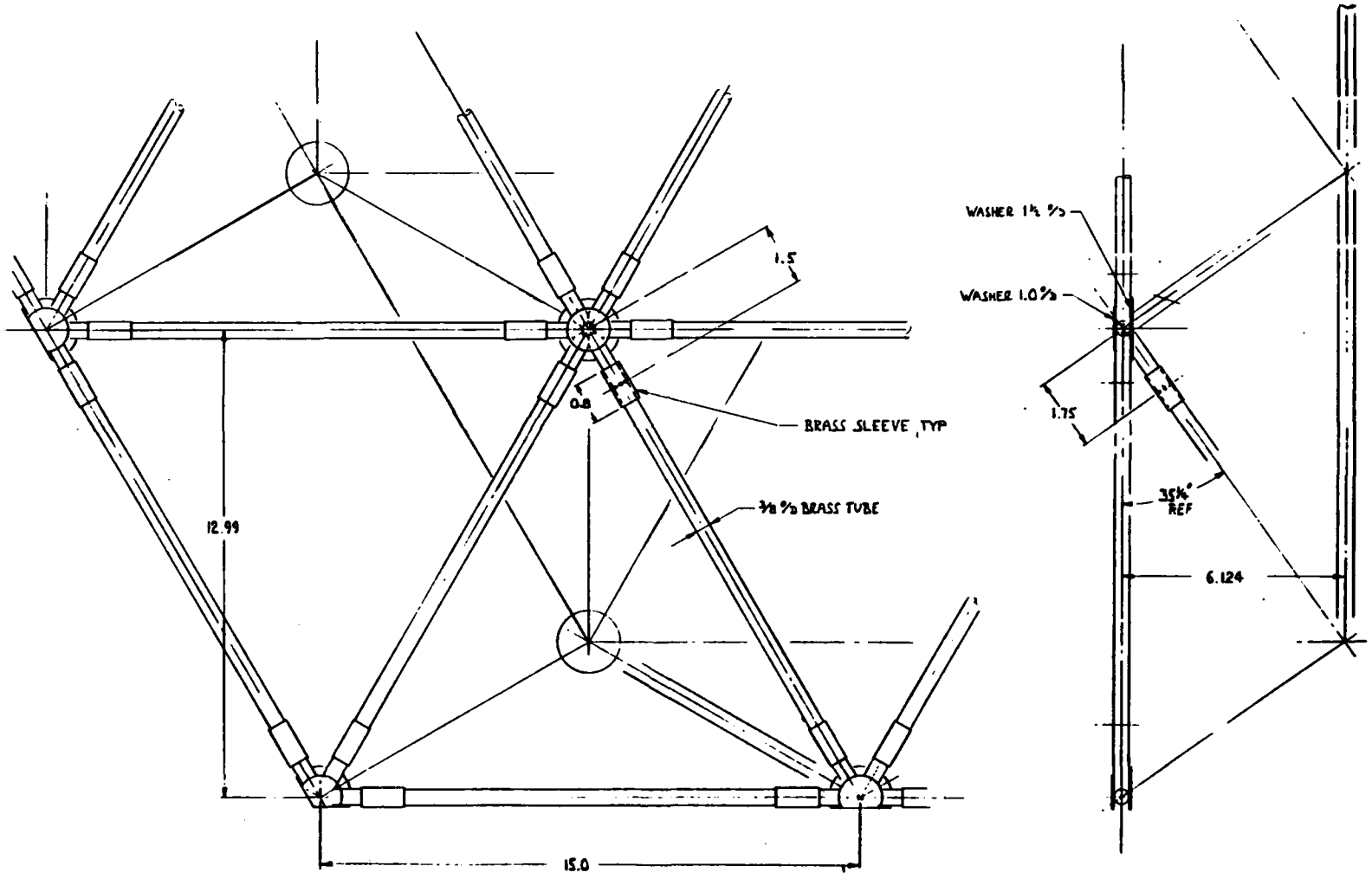

Figure 4-3. Typical Structural Detail

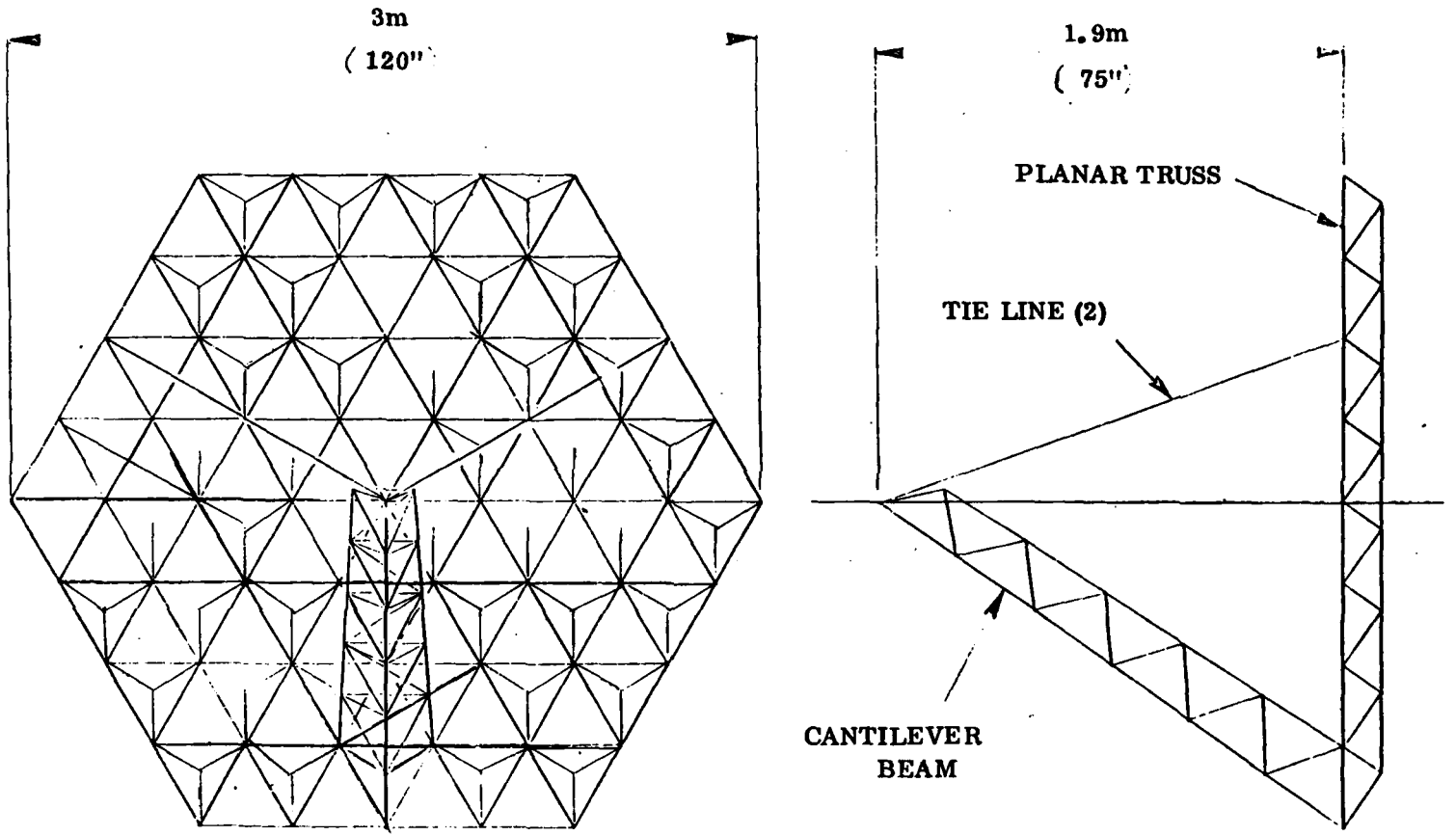

Figure 4-4. Test Article with Beam and Tension Ties

and by removing the ties, a range of overall dynamic performance is obtainable. An alternative, "braced mast" arrangement shown in Figure 4-5 represents an assembly of planar truss, pin-ended strut, and three guy lines. Modification of dynamic performance is readily accomplished by varying length of the strut and/or tension in the guy lines.

Figure 4-6 illustrates a possible structural set-up for demonstration testing that utilizes the configuration shown in Figure 4-5. The structural model is spring mounted on a dense block representing the parent spacecraft mass. Integral with the block are two tubular rods, each five feet long, representing low stiffness solar panel assemblies. Cylindrical weights are mounted on the rods to simulate the mass of the solar cells. The location of these weights on the rods is variable to enable adjustment of the dynamic response. The entire assembly is suspended by means of one or two tension ties attached to a point (or points) just above the c.g. of the assembly. The single, bifurcated suspension shown provides a degree of pendulum stability in pitch. The degree of pendulum stability in the roll direction is dependent upon the height of the point of bifurcation above the c.g. Stability in yaw is dependent on the torsion pendulum stiffness of the suspension tie. Yaw stability can be much increased by the use of two parallel suspension ties, one from each attachment point.

4.3 ACTUATOR INSTALLATION

Torque wheels were chosen for the control actuator installation studies since they are the only known device which can be used at both high and low frequencies. Control torque is generated by accelerating the rotor inertia and reacting the resulting equal but opposite torque back into the structure.

One possible torque wheel installation is shown in Figure 4-7. It can be installed on any group of three nodes anywhere on the back or front face of the structure. This "triple node" mount design permits application of bending loadings to the structure without introduction of bending loads in the individual tubular elements of the structure. The complete installation bolts directly to three node points of the demonstration structure. Torque motor loads are reacted by normal loads at the three node points and the tubular elements experience only axial loading. The support provisions consist of three bifurcated legs providing, in effect, tripod support of both the upper and lower attachment points of the actuator assembly. The trunnion-type mounting of the actuator assembly permits it to be positioned in any desired orientation about the trunnion axis. The ring plate, supporting the stator, is provided with two attachment lugs 180 degrees apart.

An alternative torque wheel installation is shown in Figure 4-8 involving only one node of the structure. Torque motor loads are reacted by bending loads in the nine tubular

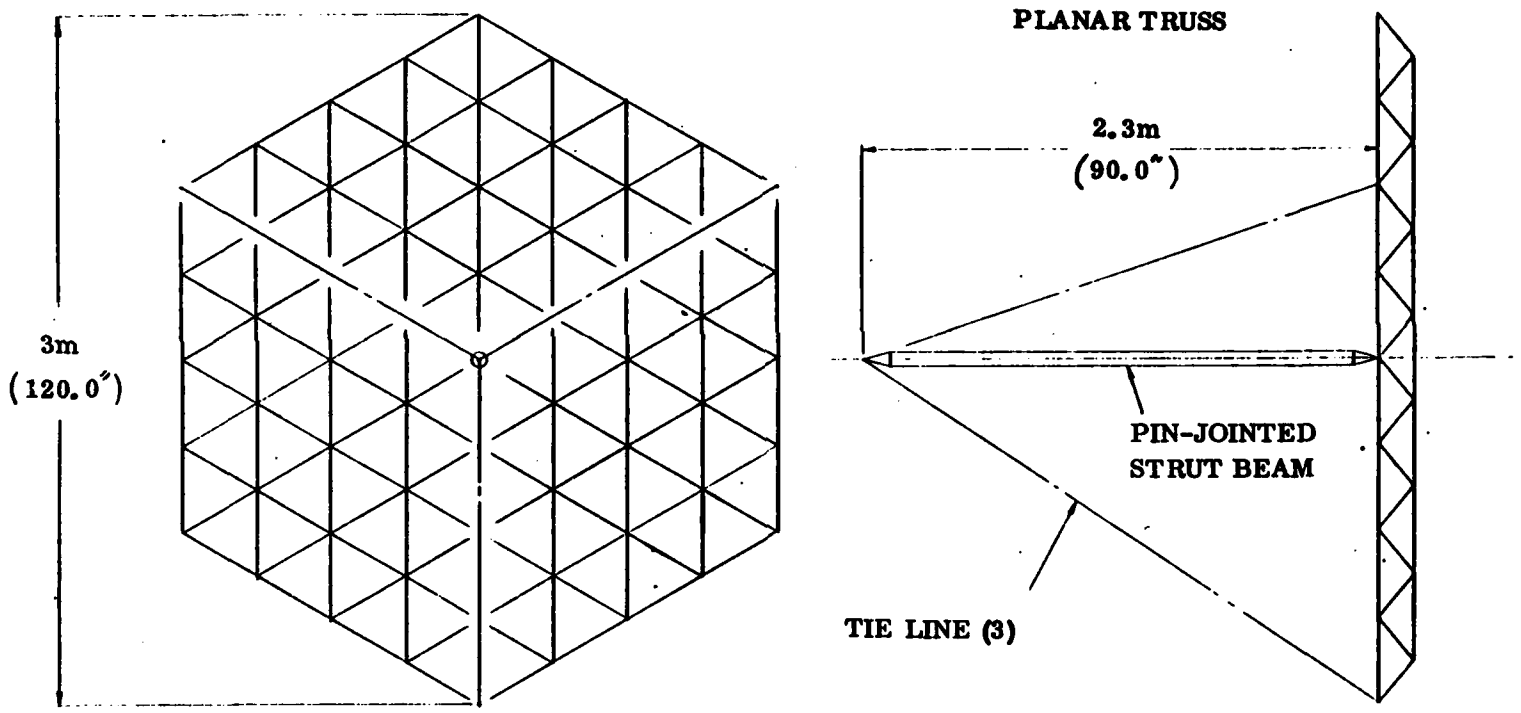

Figure 4-5. Test Article with Strut Mast and Guy Lines

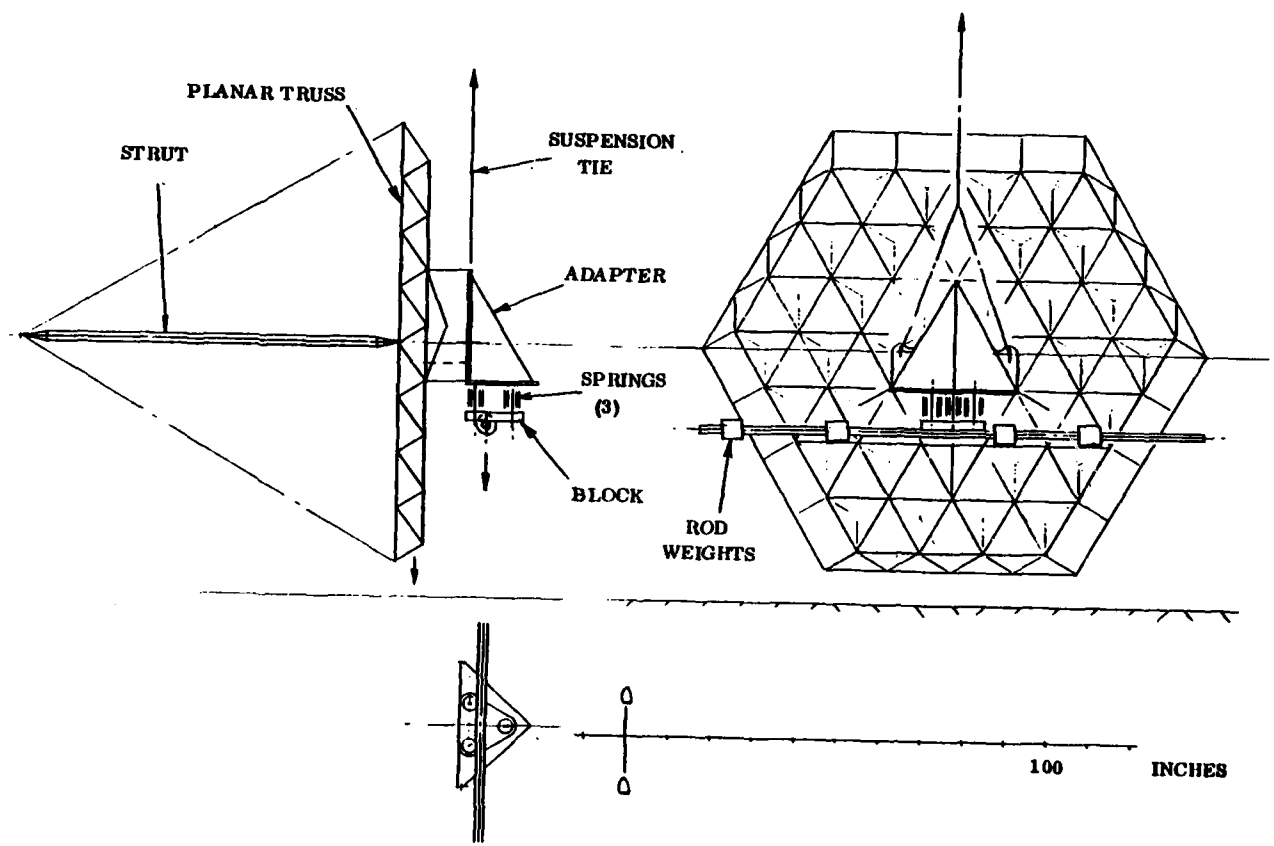

Figure 4-6. Test Installation

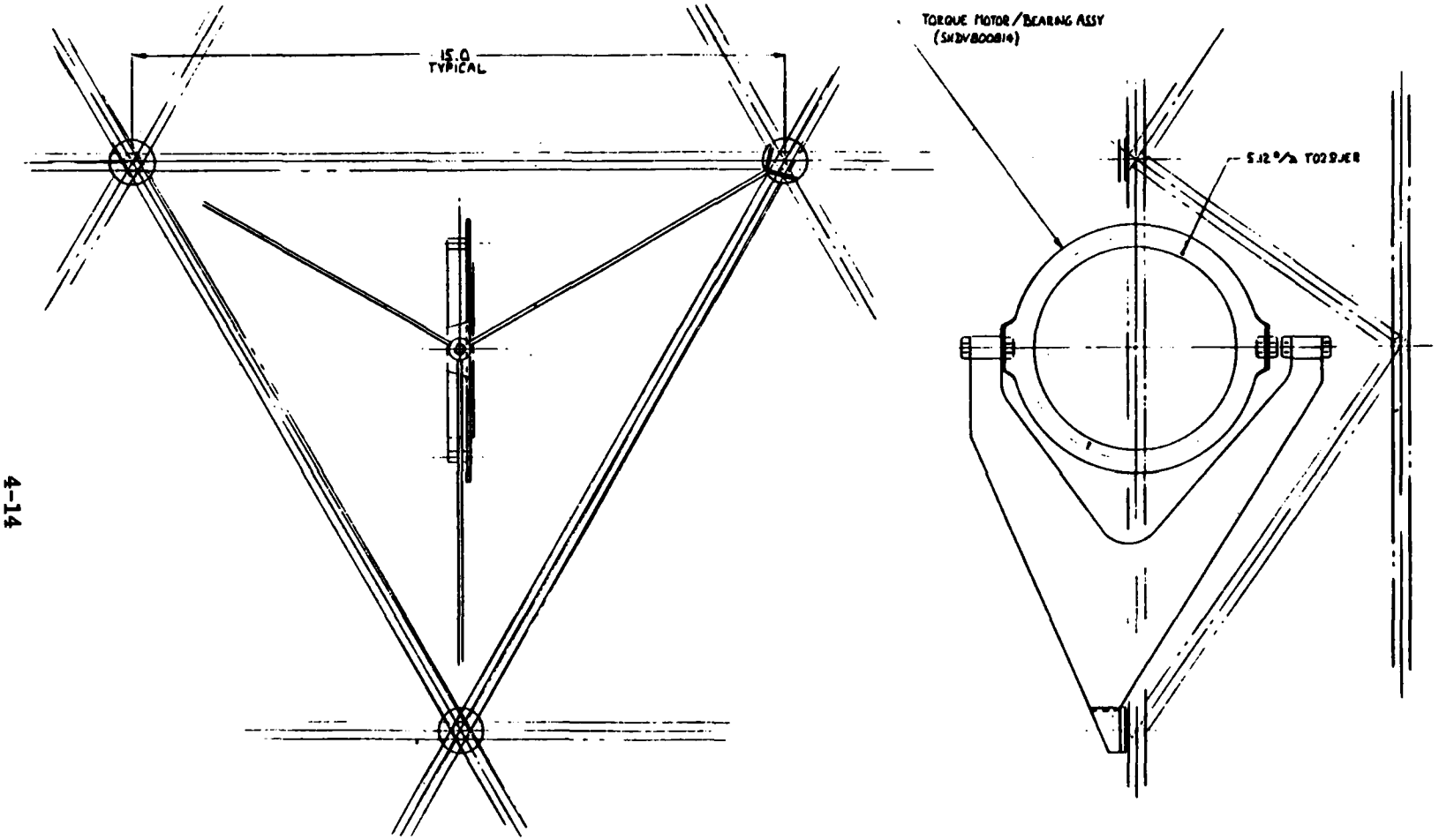

Figure 4-7. Three Node Actuator Installation

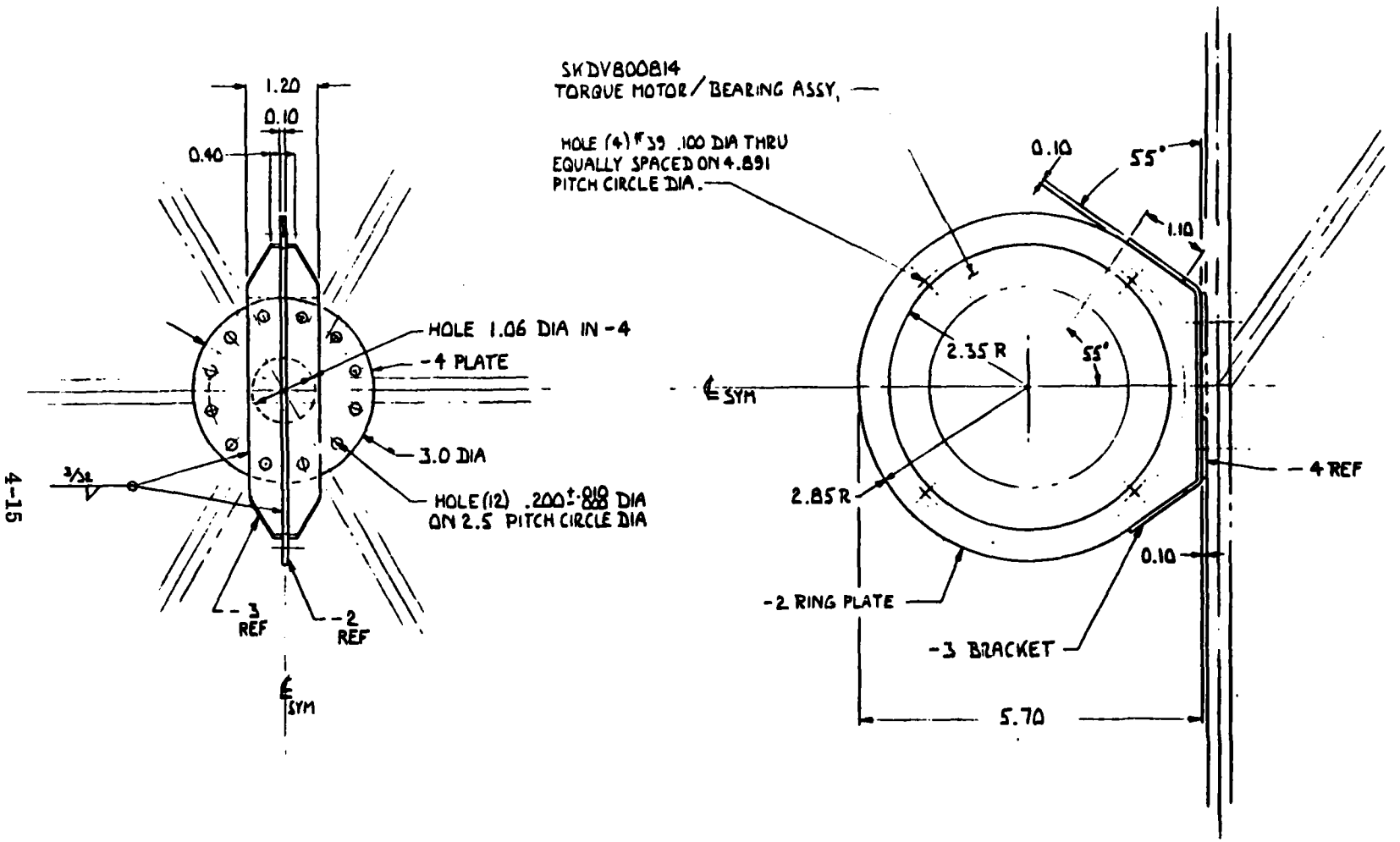

Figure 4-8. Single Node Actuator Installation

structural elements that converge at the node point. An adapter housing, consisting of an annular plate, a saddle bracket, and a circular base provides a rigid interface between the stator (outer component of the torque motor) and the structure at the node point. The circular base plate fits over the node assembly, and its circular pattern of twelve holes enables clamped attachment to the tubular elements of the structure by means of six "U" bolts. Since the twelve holes are equally spaced, the torque motor assembly may be clocked in 30^{o} increments to any preferred orientation.

SECTION 5

REFERENCES

1. S.M. Seltzer, "Attitude Control of Orbiting Large Flexible Structures: An Overview," presented at Annual Rocky Mountain Guidance and Control Conference, Keystone, CO, 1978.

2. R.E. Skelton, and P. Likins, "Techniques of Modeling and Model Error Compensation in Linear Regulator Problems," Advances in Control and Dynamic Systems, Vol. XIV, ed. C.T. Leondes, Academic Press, 1978.

3. R.R. Strunce, J.R. Lin, D.R. Hegg, P.K. Pearson, J.R. Govignon, and T.C. Henderson, ACOSS SIX (Active Control of Space Structures), Rome Air Development Center, Technical Report No. RADC-TR-80-377, January 1981.

4. R.J. Benhabib, R.P. Iwens, and R.L. Jackson, "Stability of Distributed Control for Large Flexible Structure Using Positivity Concepts," presented at AIAA Guidance and Control Conference, Paper No. 79-1780, Boulder, CO., August 6-8, 1969.

5. M. Balas, "Modal Control of Certain Flexible Dynamic Systems," Siam J. Control and Opt., Vol. 16, pp. 450-462, August 1978.

6. M. Balas, "Feedback Control of Flexible Systems," IEEE Trans. Automatic Control AC-23, pp. 673-679, 1978.

7. I.M. Horowitz, Synthesis of Feedback Systems, New York: McGraw-Hill, 1961.

8. J.R. Sesak, and P.W. Likins, "Model Error Sensitivity Suppression: Quasistatic Optimal Control for Flexible Structures," Proc. 1979 IEEE Conf. on Decision and Control, Fort Lauderdale, FL, pp. 207-213.

9. J.R. Sesak, "Control of Large Space Structures Via Singular Perturbation Optimal Control," presented at AIAA Conf. on Large Space Platforms, Paper No. 78-1690, Los Angeles, CA, September 27-29, 1978.

10. J.R. Sesak, and T. Coradetti, "Decentralized Control of Large Space Structures vis Forced Singular Perturbation," presented at AIAA Aerospace Sciences Meeting, Paper No. 79-0195, New Orleans, LA, January 15-19, 1979.

11. J.R. Sesak, P.W. Likins, and T. Coradetti, "Flexible Spacecraft Control by Model Error Sensitivity Suppression," J. Astronautical Sciences, Vol. 27, No. 2, March-April 1979.

12. J.R. Sesak, and R.V. Halstenberg, Active Control of Space Structure Phase I Report Rome Air Development Center, Technical Report No. RADC-TR-80-79, March 1980.

13. R.W. Longman, "Annihilation or Suppression of Control and Observation Spillover in the Optimal Shape Control of Flexible Spacecraft," J. Astronautical Sciences, Vol. 27, No. 4, October-December 1979.

14. J.R. Sesak, R.V. Halstenberg, Y. Chang, and M. Davis, "Filter Accommodated Optimal Control of Large Space Platforms," 2nd AIAA Conference on Large Space Platforms, Paper No. 81-0454, San Diego, CA, February 2-4, 1981.

15. B.D.O. Anderson, and J.B. Moore, Linear Optimal Control, Prentice-Hall, 1971.

16. A.E. Bryson, and Y.C. Ho, Applied Optimal Control, Blaisdell Publishing Company, Waltham, MA, 1969.

17. H. Kwakernaak, and R. Sivan, Linear Optimal Control Systems, Wiley, 1972.

18. N.K. Gupta, "Frequency-Shaped Cost Functionals: Extension of Linear-Quadratic-Gaussian Design Methods," J. Guidance and Control, Vol. 3, No. 6, pp. 529-535, November-December 1980.

19. J.C. Doyle, and G. Stein, "Robustness with Observers," Proc. 17th IEEE Conference on Decision and Control, San Diego, pp. 1-6, January 10-12, 1979.

20. J.F. Cassidy, Optimal Control with Unavailable States, Ph.D. Dissertation, Rensselaer Polytechnic Institute, Troy, N. Y., 1969.

21. A.J. Laub, "A Schur Method for Solving Algebraic Riccati Equations," IEEE Trans. Automatic Control, AC-24, pp. 913-921, December 1979.

22. D.D. Siljak, Large Scale Dynamic Systems: Stability and Structure, Elesevier - North Holland, 1978.

23. E.J. Davison, "The Feedforward Control of Linear Multivariable Time-Invariant Systems," Automatica, Vol. 9, pp. 561-573, 1973.

24. C.D. Johnson, "Accommodation of External Disturbances in Linear Regulator and Servomechanism Problems," IEEE Trans. Automatic Control, AC-16, pp. 635-644, December 1971.

25. C.D. Johnson, "Accommodation of Disturbances in Optimal Control Problems," Int. J. Control, Vol. 15, No. 2, pp. 209-231.

addresses	number of copies	line number
Richard Carman RADC/OCSE	5	
RADC/ISLD GRIFFISS AFB NY 13441	1	2
RADC/DAP GRIFFISS AFB NY 13441	2	3
ADMINISTRATOR DEF TECH INF CTR ATTN: DTIC-DDA CAMERON STA BG 5 ALEXANDRIA VA 22314	12	5
General Dynamics Convair Division P.O. Box 80847 San Diego, CA 92138	5	3
Charles Stark Draper Labs 555 Technology Square Cambridge, MA 02139	5	4
Charles Stark Draper Lab Attn: Dr. Keto Soosar 555 Technology Square M.S. -95 Cambridge, MA 02139	1	5
Charles Stark Draper Lab Attn: Dr. J.E. Linn 555 Technology Square Cambridge, MA 02139	1	6
Charles Stark Draper Lab Attn: Mr. R. Strunce 555 Technology Square M.S.-60 Cambridge, MA 02139	1	7

Charles Stark Draper Lab Attn: Dr. Daniel R. Hegg 555 Technology Square M.S. 70 Cambridge, MA 02139	1	8
ARPA/MIS 1400 Wilson Blvd Arlington, VA 22209	1	9
ARPA/SIO Attn: Lt Col A. Herzberg 1400 Wilson Blvd Arlington, VA 22209	1	10
ARPA/SIO Attn: Mr. J. Larson 1400 Wilson Blvd Arlington, VA 22209	1	11
ARPA/SIO Attn: Maj E. Dietz 1400 Wilson Blvd Arlington, VA 22209	1	12
Riverside Research Institute Attn: Dr. R. Kappesser Attn: Mr. A. DeVilliers 1701 N. Ft. Myer Drive Suite 711 Arlington, VA 22209	3	13
Riverside Research Attn: HALO Library, Mr. Bob Passut 1701 N.Ft. Myer Drive Arlington, VA 22209	1	14
Itek Corp Optical Systems Division 10 Maguire Rd. Lexington, MA 02173	1	15
Perkin Elmer Corp Attn: Mr. M. Levenstein Electro Optical Division Main Avenue Norwalk, CT 06856	1	16
Hughes Aircraft Company Attn: Mr. George Speak M.S. B-150 Culver City, CA 09230	1	17

Hughes Aircraft Company Attn: Mr. Ken Beale Centinela Teale Sts Culver City, CA 90230	1	18
Air Force Flight Dynamics Lab Attn: Dr. Lynn Rogers Wright Patterson AFB, OH 45433	1	19
AFWAL/FIBG Attn: Mr. Jerome Pearson Wright Patterson AFB, OH 45433	1	20
Air Force Wright Aero Lab. FIEE Attn: Capt Paul Wren Wright Patterson AFB, OH 45433	1	21
Air Force Institute of Technology Attn: Prof. R. Calico/ENY Wright Patterson AFB, OH 45433	1	22
Aerospace Corp. Attn: Dr. G.T. Tseng 2350 E. El Segundo Blvd El Segundo, CA 90245	2	23
Aerospace Corp. Attn: Mr. J. Mosich 2350 E. El Segundo Blvd El Segundo, CA 90245	1	24
Aerospace Corp/Bldg 125/1054 Attn: Mr. Steve Burrin Advanced Systems Tech Div. 2400 E El Segundo Blvd El Segundo, CA 90245	1	25
SD/YCD Attn: Lt Col T. May P.O. Box 92960 Worldway Postal Center Los Angeles CA 90009	1	26
SD/YCD Attn: YCPT/Capt Gajewski P.O. Box 92960 Worldway Postal Center Los Angelel, CA 90009	1	27

Grumman Aerospace Corp Attn: Dr. A. Mendelson South Oyster Bay Road Bethpage, NY 11714	1	28
Grumman Aerospace Corp Attn: Mr. Art Bertapelle Plant 25 Bethpage, NY 11714	1	29
Jet Propulsion Laboratory Attn: Mr. D.B. Schaechter 4800 Oak Grove Drive Pasadena, CA 91103	2	30
MIT/Lincoln Laboratory Attn: S. Wright P.O. Box 73 Lexington, MA 02173	1	31
MIT/Lincoln Laboratory Attn: Dr. D. Hyland P.O. Box 73 Lexington, MA 02173	11	32
MIT/Lincoln Laboratory Attn: Dr. N. Smith P.O. Box 73 Lexington, MA 02173	11	33
Control Dynamics Co. Attn: Dr. Sherman Seltzer 221 East Side Square, Suite 1B Huntsville, Al 35801	1	34
Lockheed Space Missile Corp. Attn: A. Woods, Bldg 130 Organ 62-E6 3460 Hillview Ave Palo Alto, CA 94304	2	35
Lockheed Missiles Space Co. Attn: Mr. Paul Williamson 3251 Hanover St. Palo Alto, CA 94304	1	36

General Dynamics Attn: Ray Halstenberg Convair Division 5001 Keary Villa Rd San Diego, CA 92123	1	37
STI Attn: Mr. R.C. Stroud 20365 Stevens Creek Blvd. Cupertiono, CA 95014	1	38
NASA Langley Research Ctr Attn: Dr. G. Horner Attn: Dr. Card Langley Station Bldg 1293B M/s 230 Hampton, VA 23665	2	39
NASA Johnson Space Center Attn: Robert Piland Ms. EA Houston, TX 77058	1	40
McDonald Douglas Corp Attn: Mr. Read Johnson Douglas Missile Space Systems Div 5301 Bulsa Ave Huntington Beach, CA 92607	1	41
Integrated Systems Inc. Attn: Dr. Narendra Gupta 151 University Ave. Suite 400 Palo Alto, CA 94301	1	42
Boeing Aerospace Company Attn: Mr. Leo Cline P.O. Box 3999 Seattle, WA 98124 MS 8 H-23	1	43
TRW Derense Space Sys Group Inc. Attn: Ralph Iwens Bldg 82/2054 One Space Park Redondo Beach, CA 90278	1	44
TRW Attn: Mr. Len Pincus Bldg R-5, Room 2031 Redondo Beach, CA 90278	1	45
Department of the navy Attn: Dr. K.T. Alfriend Naval Research Laboratory Code 7920 Washington, DC 20375	1	46

Airesearch Manuf. Co. of Calif. Attn: Mr. Oscar Buchmann 2525 West 190th St. Torrance, CA 90509	1	47
Analytic Decisions, Inc. Attn: Mr. Gary Glaser 1401 Wilson Blv. Arlington, VA 22209	1	48
Analytic Decisions, Inc. Attn: Mr. Richard Mollicone 5336 West Rosecrans Ave Suite 203 Lawndale, CA 22209	1	49
Center for Analysis Attn: Mr. Jim Justice 13 Corporate Plaza Newport Beach, CA 92660	1	50
General Research Crop. Attn: Mr. J. R. Curry P.O. Box 3587 Santa Barbara, CA 93105	1	51
General Research Corp Attn: Mr. Thomas Zakrzewski 7655 Old Springhouse Road McLean, VA 22101	1	52
Institute of Defense Analysis Attn: Dr. Hans Wolfhard 400 Army Navy Drive Arlington, VA 22202	1	53
Karman Sciences Corp. Attn: Dr. Walter E. Ware 1500 Garden of the Gods Road P.O. Box 7463 Colorado Springs, CO 80933	1	54
MRJ, Inc. 10400 Eaton Place Suite 300 Fairfax, VA 22030	1	55

Rhoton Research Associates
Attn: Mr. Jim Myer
P.O. Box 1318
La Jolla, CA 92038

1 56

Rockwell International

1 57

Attn: Russell Loftman (Space Systems Group)
(Mail Code - SL56)
12214 Lakewood Blvd.
Downey, CA 90241

Science Applications, Inc.
Attn: Mr. Richard Ryan
3 Preston Court
Bedford, MA 01730

1 58

U.S. Army Missile Command
Attn: DRSMI-RAS/Mr. Fred Haak
Redstone Arsenal, AL

1 59

Naval Electronic Systems Command
Attn: Mr. Charles Good
PME_106-4
National Center I
Washington, DC 20360

1 60

Naval Research Laboratory
Attn: Dr. John McCallum
E07P0
4555 Overlook Ave., SW
Washington, DC 20375

1 61

U.S. Army/DARCOM
Attn: Mr. Bernie Chasnov
AMC Bldg
5001 Eisenhower Ave
Alexandria, VA 22333

1 62

Honeywell Inc.
Attn: Dr. Thomas B. Cunningham
Attn: Dr. Michael F. Barrett
2600 Ridgway Parkway MN 17-2375
Minneapolis, MN 55413

2 65

MISSION
of
Rome Air Development Center

RADC plans and executes research, development, test and selected acquisition programs in support of Command, Control Communications and Intelligence (C^3I) activities. Technical and engineering support within areas of technical competence is provided to ESD Program Offices (POs) and other ESD elements. The principal technical mission areas are communications, electromagnetic guidance and control, surveillance of ground and aerospace objects, intelligence data collection and handling, information system technology, ionospheric propagation, solid state sciences, microwave physics and electronic reliability, maintainability and compatibility.